UNIVERSITY OF NAPLES FEDERICO II

PH.D. PROGRAM

IN

CLINICAL AND EXPERIMENTAL MEDICINE

CURRICULUM IN TRANSLATIONAL MEDICAL SCIENCES

XXXV Cycle
(Years 2019-2022)

Chairman: Prof. Francesco Beguinot

PH.D. THESIS

TITLE

Glucose promotes breast cancer cell stemness and invasiveness by modulating the interaction with mammary adipose tissue-derived mesenchymal stem cells

TUTOR

Prof. Pietro Formisano

PH.D.STUDENT

Dr. Teresa Migliaccio

Table of contents

List of Publications

Maria Rosaria Ambrosio, Giusy Mosca, **Teresa Migliaccio**, Domenico Liguoro, Gisella Nele, Fabrizio Schonauer, Francesco D'Andrea, Federica Liotti, Nella Prevete, Rosa Marina Melillo, Carla Reale, Concetta Ambrosino, Claudia Miele, Francesco Beguinot, Vittoria D'Esposito, Pietro Formisano. Glucose Enhances Pro-Tumorigenic Functions of Mammary Adipose-Derived Mesenchymal Stromal/Stem Cells on Breast Cancer Cell Lines. Cancers (Basel). 2022 Nov 3;14(21):5421.

Maria Rosaria Ambrosio, Elisa Magli, Giuseppe Caliendo, Rosa Sparaco, Paola Massarelli, Vittoria D'Esposito, **Teresa Migliaccio**, Giusy Mosca, Ferdinando Fiorino, Pietro Formisano. Serotoninergic receptor ligands improve Tamoxifen effectiveness on breast cancer cells. BMC Cancer. 2022 Feb 15;22(1):171.

Vittoria D'Esposito, Manuela Lecce, Gaetano Marenzi, Serena Cabaro, Maria Rosaria Ambrosio, Gilberto Sammartino, Saverio Misso, **Teresa Migliaccio**, Pasquale Liguoro, Francesco Oriente, Leonzio Fortunato, Francesco Beguinot, José Camilla Sammartino, Pietro Formisano, Roberta Gasparro. Platelet-rich plasma counteracts detrimental effect of high-glucose concentrations on mesenchymal stem cells from Bichat fat pad. J Tissue Eng Regen Med. 2020 May;14(5):701-713.

1.Introduction

1.1 Diabetes and cancer

The International Diabetes Federation has estimated that the number of people with diabetes is expected to rise from 425 million adults in 2017 to 629 million by 2045. Diabetes mellitus (DM) has become one the most pressing and prevalent issue in the last few decades, hand-in-hand with the rising obesity crisis. It is now the seventh leading cause of death in the USA as well as worldwide, with about 5.2 million annual deaths globally attributed to diabetes (1). There are three types of DM in the form of type 1, type 2, and gestational diabetes. Gestational DM occurs during the second or third trimester of pregnancy, increasing the future risk of those patients to type 2 DM with an incidence of 35–60% in the two decades after delivery or a 7.4-fold increased risk (2,3). Type 1 and type 2 diabetes (T1D and T2D) are both common chronic diseases affecting millions of people worldwide, leading to poor health outcomes and increased healthcare costs (4). In addition, both diseases (T1D and T2D) are associated with reduced quality of life (5). T1D, which accounts for only 5–10% of those with diabetes, previously encompassed by the terms insulin-dependent diabetes or juvenile-onset diabetes, results from cellular-mediated autoimmune destruction of the beta cells of the pancreas.

Type 2 diabetes (T2D) and its comorbidities have reached epidemic proportions. The prevalence and incidence of T2D, representing >90% of all cases of diabetes, are increasing rapidly throughout the world (6). Two major pathophysiological mechanisms characterize T2D: insulin resistance, especially in skeletal muscle and liver, and defective insulin secretion from the pancreas (7). The risk factors for T2D include those associated with lifestyle, such as unhealthy eating, as well as genetic factors that interact with each other and an individual's living environment (8). T2D may be associated with increased risk, accelerated progression and greater mortality rates of several types of cancer, such as liver, pancreatic, endometrial, colorectal and breast cancer. Cancer and diabetes are prevalent diseases that significantly affect global health. Epidemiologic data

indicate that diabetic individuals are at a substantially higher risk of developing cancer (9,10,11). The Emerging Risk Factors Collaboration investigators demonstrated that individuals with confirmed diabetes had a significantly higher risk of cancer death than people without diabetes, based on a pooled analysis of 97 prospective cohort investigations involving approximately 800,000 participants (12). Numerous biological associations exist linking diabetes and a higher risk of cancer. Metabolic disturbances in diabetes may be associated with cancer incidence, progression, aggressiveness and response to treatment. Alterations in body mass (obesity) and the levels of adipocytokines, but also increased growth factors and hormone levels and inflammation are implicated in cancer pathophysiology observed in diabetes. Thus, dyslipidemia, hyperinsulinemia and hyperglycemia are the three main metabolic disturbances that occur in diabetes. Therefore, in a diabetic individual, the effects of increased lipids, altered insulin levels, its action and hyperglycemia can be considered as triggers to cancerous phenotypes in diabetes (Figure 1).

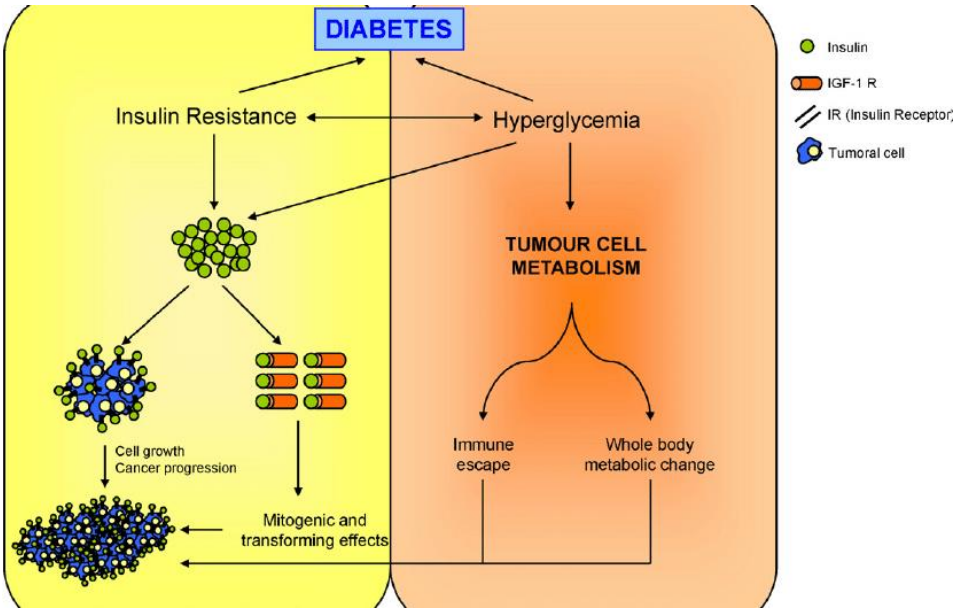

Figure 1. Associated-diabetes metabolic alterations promote cancer development.

1.2 Diabetes and breast cancer

Breast cancer (BC) is the most common malignancy in women worldwide (13). Among the different forms of cancer, several studies have reinforced a link between breast cancer risk and diabetes (14,15). Global breast cancer (BC) incidence has increased over the last three decades (16). Female breast cancer has overtaken lung cancer as the most commonly diagnosed cancer, with a total of 2.26 million cases in the year 2020 (17). Despite the steadily decreasing mortality rate of breast in high-resource countries, breast cancer remains as the leading cause of cancer deaths for women worldwide (18). It was estimated that more than one million women would die of breast cancer in the year 2040 (19). Associations between T2DM and breast cancer have been intensely studied, particularly regarding diabetes and the risk and prognosis of breast cancer (20). Diabetes is associated with a 14% to 25% increased risk of breast cancer and a 37% to 61% elevated hazard of all-cause mortality in breast cancer patients (21).

1.3 Diabetes and breast cancer: role of hyperglycemia

Hyperglycemia is associated with a higher incidence of breast cancer (22). Several meta-analyses studies regard the association between hyperglycemia, diabetes, and BC; however, the exact mechanisms are not well understood (23). Overall, the data suggest that patients with hyperglycemia or pre-existing diabetes have a decreased overall survival and disease-free survival (24). Breast cancer has several known risk factors, including age, sex, obesity, estrogen levels, and family history (25). Recent studies have shown that hyperglycemia is an important risk factor in the development of BC (26). In BC, hyperglycemia is associated with an increased prevalence and mortality, but also significantly impacts the efficacy of chemotherapy and can lead to chemoresistance. Hyperglycemia has been linked to increased cancer cell proliferation, inhibited cancer cell apoptosis and increased cancer metastasis. In diabetes, hyperglycemia results from increased systemic insulin resistance (27). Indirect effects of hyperglycemia on cancer cells are mediated by an increase in the circulating levels of insulin/IGFs, by the increase in the inflammatory cytokines such as IL-6 and TNFa, through the generation of

reactive oxygen species (ROS; oxidative stress) and platelet activation. The "Warburg" effect is considered an important feature of glucose metabolism in tumours (28). Under hypoxic conditions, aerobic glycolysis in tumour cells significantly changes compared to aerobic oxidation. Thus, cancer cells upregulate the processes of glycolysis and the catabolism of glucose to form lactate. This process is accompanied by ATP production. However, ATP produced by glycolysis is insufficient to support the survival of cancer cells, so the rate of glucose uptake and the fermentation of glucose to lactate are both increased. A sufficient energy supply activates cellular signalling pathways, promotes the abnormal activity of tumour cells, and induces an anti-apoptotic response and chemotherapy resistance. The reprogramming of glucose metabolism accelerates the conversion of glycolysis and changes the microenvironment's acidity, which promotes the expression of angiogenic factors and enhances tumour metastasis (29). High glucose levels in the microenvironment are very important in tumour growth. Hyperglycemia induces changes in the microenvironment, such as an increase in pH, a high concentration of lactic acid, the production of inflammatory factors, the imbalance of ROS, and the impact on adipose and immune cells (Figure 2). The impact of a modified tumour microenvironment on cancer cells is thought to result in tumour relapse, therapeutic resistance, and metastasis (30).

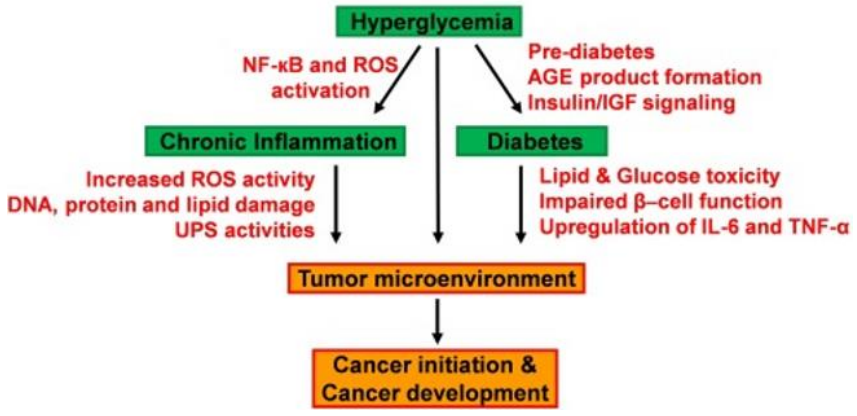

Figure 2. Hyperglycemia favours cancer initiation and development, inducing changes in the tumor microenvironment.

1.4 (Breast) Cancer Stem Cells

The cellular origin of cancer remains an important and central question. Cancer is a group of diseases characterized by the dysregulation of important pathways, that control cellular processes involved in DNA repair, cell survival, proliferation and mortality (29). Cell transformation, tumor progression and metastasis are orchestrated by a complex and intriguing network of interactions, where genomic and epigenomic mutations, especially in oncogenes and tumour suppressor genes, and environmental factors induce malignancy and tumorigenesis (30). Several studies reported that many women still show drug resistance and tumor relapse after an initial response to the chemotherapies and recurrent form of breast cancer remains to be incurable. Aggressiveness and drug resistance seem to be due to a minute population of cancer cells known as cancer stem cells (CSCs), which show self-renewal, differentiation properties and tumorigenic potential. Two separable but closely related hypotheses explain the tumor heterogeneity and origin of CSCs. According to clonal evolution or stochastic model, all the cells in the tumor have a similar tumorigenic potential and tumor heterogeneity depends on the generation of intratumoral clones through sequential mutations. This model presumes that CSCs can be generated from differentiated mammary cells due to mutations, that occur during the disease. Exposure to environmental factors such as radiation and chemotherapies induces genetic alterations in non-malignant somatic cells that prime the de novo generation of CSCs by the de-differentiation process (31). Several reports also suggest that microenvironmental cues induce the malignant transformation of differentiated cells into BCSCs. The hierarchical or CSC model postulates that only a small proportion of tumor cells resident in the tumor has a tumor-propagating potential. These cells exhibit self-renewal properties and can reiterate tumor hierarchy (Figure 3) (32).

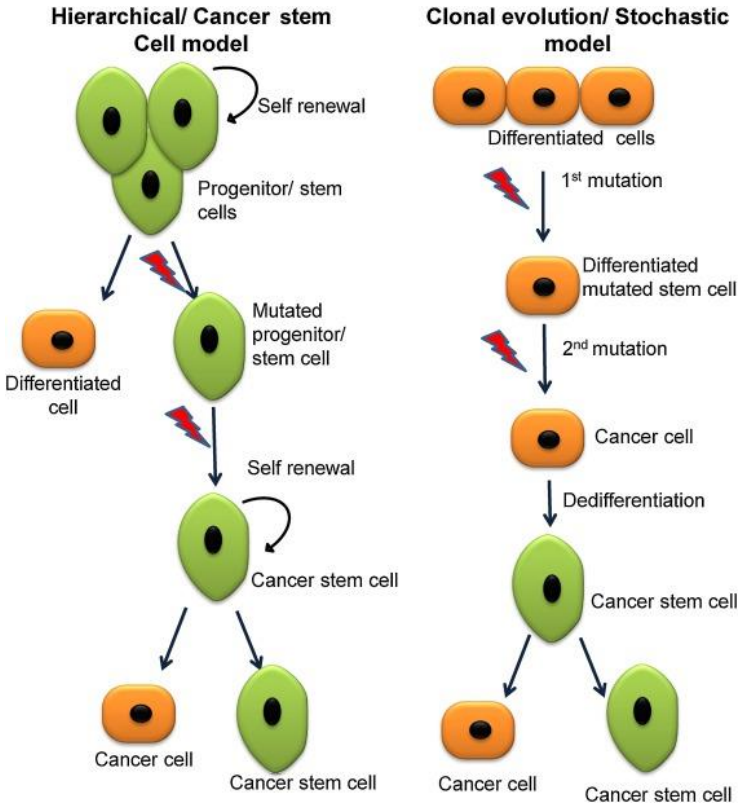

Figure 3. Origin of CSCs. CSC model states that a minute population of cells possesses self-renewal and differentiation capacities, and tumorigenic potentials. These self-renewal and differentiation capabilities contribute to tumor heterogeneity. Clonal evolution model states that BCSCs can be generated from differentiated mammary cells by dedifferentiation process. Tumour heterogeneity is due to the formation of intra-tumoral clones by sequential mutations.

The CSCs are defined as a subpopulation of tumor cells with the capacity for self-renewal and differentiation to drive the initiation, progression, metastasis and recurrence of tumor. CSCs exhibit anti-cancer treatment resistance, that can avoid being killed by conventional chemo-and radio-therapies, as well as the properties to remain viable and to enable the re-establishment of tumors. The most common way to identify CSCs is through investigating the expression of characteristic cell surface markers. The development of CSC-specific biomarkers has facilitated the identification and validation of the same in *in vitro* and *in vivo* breast cancer models and patients. The molecular markers which are used for identification and validation are CD44, CD24, ALDH1, and CD133 (33). CD44 is a cell surface glycoprotein, which plays a prominent role in cell signaling, adhesion and migration. Several studies suggest that it regulates cancer cell proliferation, angiogenesis and metastasis (34). CD24 is an adhesion glycoprotein expressed on

the surface of many cell types, and it's a recently discovered ligand for P-selectin. The CD24 expression is found in highly differentiated tumor cells (luminol-type) (35). Higher expression of CD44 and lower expression of CD24 mark the CSC population (36). The combination of CD44 and CD24 expression has been extensively used as a breast cancer stem cells marker (BCSC). Breast tumor-derived $CD44^{+}/CD24^{-}$ cells are able to form tumors when implanted into immunosuppressed mice. Breast tumor with expression of $CD44^{+}/CD24^{-}$ markers have been shown to exhibit enhanced invasion and metastasis (37). ALDH1 is also a marker of CSCs. The activity of ALDH1 in cells is associated with stem cell phenotype and its expression is associated with poor clinical outcomes in breast cancer. The ALDH1 expression is also linked to drug resistance in breast cancer (38). CD133 also acts as a CSC-specific marker in triple-negative breast cancer and BRCA1 mutant tumors. The mechanism underlying the differential expression of $CD44^{+}/CD24^{-}$ and ALDH1 in breast cancer has not been found yet. Analogies between stem cells and cancer stem cells can be drawn on many levels. Both show the ability of self-renewal and heterogeneity and share signalling pathways commonly associated with the replication of stem cells such as Wnt, Bcl2, Sonic Hedgehog and Notch (39). Wnt is a glycoprotein that serves as a ligand for Frizzled (FZD), a seven serpentine transmembrane receptor and low-density receptor-related protein 5/6 (LRP5/6). Accumulating evidence suggests that Wnt signalling has a prominent role in orchestrating CSC self-renewal and differentiation. Aberrant regulation of Wnt increases niche-independent and deviant differentiation of stem cells (40). The Notch is an essential transmembrane signalling receptor required throughout embryogenesis and involved in determining stem cell fate, cell differentiation, apoptosis and cell cycle progression. Expression of Notch signalling components (JAG 1, Notch 1 and Notch 4) is very common in breast cancer and also associated with poor patient's survival. Notch signalling participates in breast tumorigenesis certainly by maintaining BCSC phenotype (41). Higher Notch activation leads to increased sphere formation and higher expression of stemness genes, including *OCT4, NANOG, SOX2, ALDH* and *KLF4* (42). Hedgehog (HH) signalling plays an important role in various cellular processes during embryonic development and

tissue homeostasis and is also a key regulator of cell fate and self-renewal (43). Hyperactivation of this pathway, by either mutation or deregulation, has recently been recognized to cause tumorigenesis in various tissues. The most interesting, and still evolving concept, involves the association of Hh signalling with CsCs (44).

In addition, expression of stem cell-specific transcription factors like OCT4, SOX2 and NANOG has also been observed in breast cancer stem cells (45). OCT4, SOX2, and NANOG are critical regulators of self-renewal and pluripotency of embryonic stem cells and regulate cell proliferation and differentiation. Clinical studies have shown that tumors with intense OCT4 stem cell marker expression are associated with further disease progression, greater metastasis, and shorter cancer-related survival compared to tumors with moderate and low OCT4 expression (46). Furthermore, OCT4 is reported to be a core regulator of stem cell self-renewal and differentiation and was recently validated as a CSCs target (47). It was observed that overexpression of OCT4 and NANOG enhances spontaneous changes in the expression of EMT-related genes in CSCs and promotes CSCs invasiveness. Such suggested that OCT4 and NANOG could be markers of poor prognosis (48). Another important feature of CSC is the ability to form spheres in an *in vitro* system. Identification and isolation of CSCs through cultivation of tumoral spheres consist in observing the capacity of tumoral cells to grow in suspension in ultra-low attachment plates. This method is very important and useful for evaluating the self-renewal ability of cancer cells (49). Dontu et al. have developed an *in vitro* cultivation system, that allows the propagation of human mammary epithelial cells in an undifferentiated state based on their ability to proliferate in suspension as" nonadherent mammospheres". They demonstrated that nonadherent mammospheres are enriched in early progenitor stem cells, which can differentiate along three mammary epithelial lineages and clonally generate complex functional structures in reconstituted 3D culture systems (50). *In vitro* 3D culture system has received much attention in the field of biomedicine due to its ability to mimic tissue structure and function, allowing communication and cellular interaction. This system proved to be useful for selection and

propagation of tumorogenic breast cancer cells from primary tumor and metastasis and even as a tool to screen new drugs targeting CSCs.

1.5 Tumor microenvironment and breast cancer: the importance of adipose tissue

Numerous studies have evidenced that tumor microenvironment plays a significant role during breast cancer development and progression. Mittal et al. demonstrated the dependency of breast tumor cells on different components of the microenvironment for their survival, dissemination, dormancy and establishment in secondary sites to form metastasis, as well as the potential as a therapeutic target to improve breast cancer outcome (51). Breast tumour comprises proliferating epithelial-derived cancer cells supported by various non-cancerous stromal components, often collectively referred to as 'the tumour microenvironment'. These include fibroblasts, immune cells, endothelial cells, infiltrating inflammatory cells, adipocytes, as well as signalling molecules and extracellular matrix (ECM) components (52). Breast tumor microenvironment is largely composed of adipose tissue (AT) with important interaction between epithelial cells and adipose cells. Adipose tissue is a loose connective tissue characterized by marked cellular heterogeneity. It comprises about one-third of adipocytes and two-thirds of stromal-vascular fraction cells, a combination of Mesenchymal Stem Cells (MSC), endothelial precursor cells, fibroblasts, smooth muscle cells, pericytes, macrophages and preadipocytes in various stages of development (53). Adipose tissue is now accepted as an endocrine organ, that produces and secretes numerous hormones, growth factors, matrix proteins, enzymes, cytokines, and complement factors. The secreted factors identified play a role in fat mass regulation and adipocyte differentiation, vascular and blood flow regulation, lipid and cholesterol metabolism, and immune system function (54). Over 350 proteins have been identified in mammary AT and these factors are called "adipokines"; they are very important to maintain glucose and energy homeostasis and include leptin, adiponectin, resistin, growth factor (IGF1, insulin-like growth factor 1; VEGF, vascular endothelial growth factor; EGF, epidermal growth factor; FGF, fibroblast growth factor; TGFβ, transforming growth factor), enzymes (autotaxin)

and cytokines (interleukin [IL]-1, IL-6, IL-8, CCL5, tumor necrosis factor-TNF-α). These molecules are crucial for the physiology and development of AT, breast epithelium, and the entire organism (55). Breast adipose tissue is a rich energy source, that plays a major role in breast development and maturation. Several studies demonstrated that adipose tissue aids the development and progression of BC through the secretion of growth factors and cytokines, utilized by cancer cells for survival (56). Metabolic disorders associated with diabetes, such as hyperglycemia, can alter the metabolic profile of adipose tissue and lead to increased secretion of numerous hormones, adipokines, inflammatory cytokines, enzymes and free fatty acids. Adipose tissue-specific secreted factors contribute to the initiation and progression of breast cancer (Figure 4). Recent studies in vitro showed that adipocytes might integrate inputs from the metabolic environment, like high glucose and high fatty acid concentrations, and release factors, like IGF-1, the chemokine CCL5 and interleukin 8 (IL-8), promoting proliferation, migration and invasiveness and chemoresistance of breast cancer cells (57,58,59).

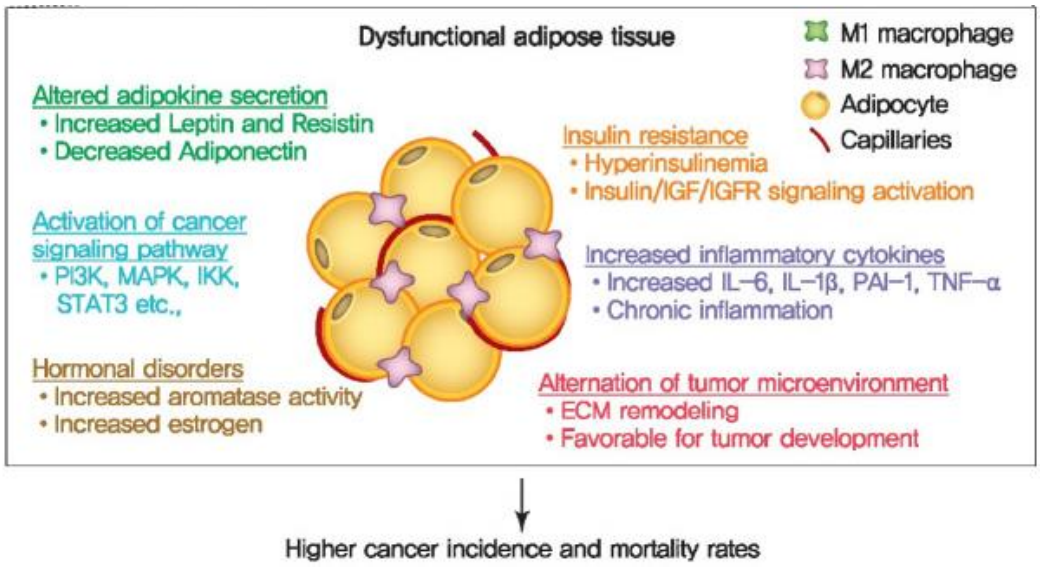

Figure 4. Metabolic disorders in adipose tissue contribute to the initiation and progression of cancer by producing endocrine and paracrine factors and alternation of tumor microenvironment.

1.6 Mesenchymal stem cells: role in tumor progression

Mesenchymal stem cells (MSCs) are an important component of the tumor microenvironment (TME). MSCs are non-hematopoietic precursors initially

isolated from the bone marrow as adherent, highly proliferating elements with long-term self-renewal potential and multilinear differentiation into different tissues of mesenchymal origin (60). MSCs can be obtained from different tissues, e.g., bone marrow, adipose tissues, placenta or umbilical cord and can be propagated to give rise to cellular products that are used for therapy. MSCs are also referred to as "mesenchymal stromal cells." This nomenclature acknowledges the origin of MSCs from the stromal compartment and implies that mesenchymal stromal cells have properties associated with stem cells. MSCs are a population of adult multipotent cells capable of self-renewal and differentiation into osteoblasts, chondrocytes and adipocytes (61). The facility of isolating and cultivating them and their high potential for ex vivo expansion make MSCs an interesting resource, that can be used for a wide range of clinical applications in the context of cell and gene therapy and in regenerative medicine (62). MSCs have been reported to contribute to tissue repair through differentiation, cell fusion or the secretion of cytokines and growth factors (63). MSCs are cells potentially capable of differentiating not only into tissues of mesenchymal origin, including medullary stroma, adipose tissue, bone, and cartilage, but also into cells of non-mesodermal origin such as neurons, skin and digestive tract epithelial cells, liver and lung (64) (Figure 5).

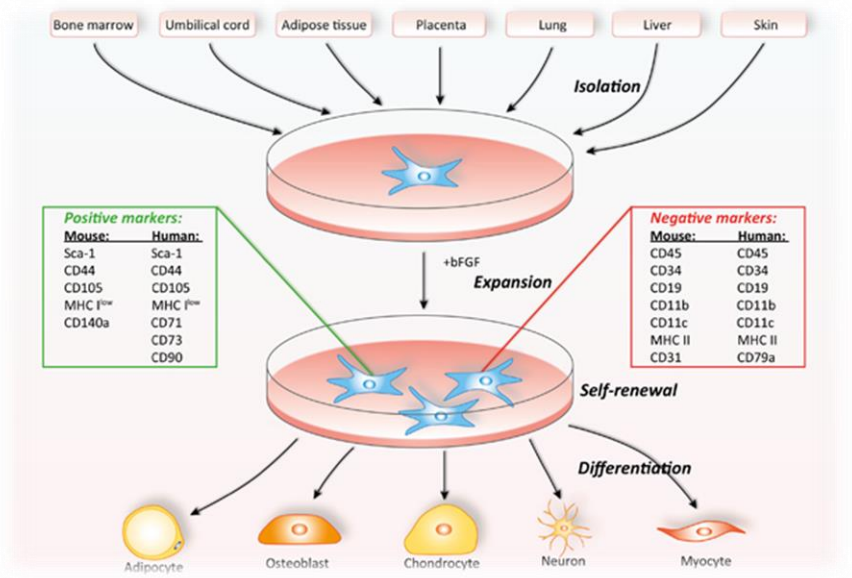

Figure 5. Isolation, expansion and differentiation of mesenchymal stem cells.

Because of their self-renewal capacity, multi-potency and immunomodulatory properties, MSCs have become an attractive tool for regenerative medicine. Currently, they serve as a major cellular source for replacing damaged tissues or pathological lesions (65-66). MSCs play a crucial role in tumor progression. Numerous evidence demonstrated that MSCs promote tumor development, progression and relapse in different cancers, including breast cancer. Cancer cells and Mesenchymal stem cells can establish reciprocal interactions, inducing transcriptional, secretory and phenotypic modifications that promote neoplastic progression. They provide a framework for anchoring tumor cells in the form of tumor stroma and secrete factors that facilitate tumor growth (67). It was discovered that MSCs secrete multiple bioactive factors, that can dramatically alter the key cellular functions of neighbouring cells, such as survival, apoptosis, maturation and differentiation (68). Several studies have revealed that MSCs have tumor-supporting paracrine activities. Several cytokines, involved during MSC-mediated tissue regeneration (e.g. IL-6, TGFβ, VEGF), are secreted at elevated levels by MSCs upon recruitment by cancer cells and actively support growth or invasion of cancer cells. MSCs release IL-6, which supports tumor growth by stimulating cancer cell proliferation and survival or protecting them from apoptosis. In addition, they could also potentiate cancer cell migration, invasion, and metastasis via the release of IL-6 in the tumor microenvironment (69). Mesenchymal stem cells can also secrete a combination of anti-apoptotic and angiogenic factors (70-71), including HGF, SDF-1/CXCL12, CD106 (sVCAM) and VEGF, which can promote tumor growth, local angiogenesis and metastasis. MSCs have also been shown to release elevated levels of TGFβ upon interaction with breast and prostate cancer (72-73), resulting into stimulation of the proliferative and migratory capacities of the cancer cells. The implication of TGFβ signalling in promotion of tumor invasion and metastasis via EMT is well established (74). Another MSC-secreted cytokine, CCL5 (RANTES), is associated with tumor progression and invasion in various cancers. CCL5 can be secreted by MSC and displays pro-proliferative activities on breast cancer cell lines (75). Other MSCs-secreted factors are upregulated during interactions with cancer cells

and exhibit a potent effect on tumor cells including BMP2, CXCL1, CXCL5, CXCL6, CXCL7, EGF, IL4, IL8, IL10, IL17b or S100A4.

1.7 Cancer-associated fibroblasts (CAFs) and senescent cells in tumor progression

Fibroblasts are non-vascular, non-epithelial and non-inflammatory cells of the connective tissue and are its principal cellular component. The important functions of fibroblasts include the deposition of extracellular matrix (ECM), regulation of epithelial differentiation, regulation of inflammation, and involvement in wound healing (76). Fibroblasts synthesize some constituents of the fibrillar Extra Cellular Matrix, contributing to the formation of basement membranes (77). In addition, fibroblasts are important in maintaining of homeostasis of adjacent epithelia through the secretion of growth factors and direct mesenchymal–epithelial cell interactions. The fibroblasts within the tumour stroma acquire a modified phenotype; they start to proliferate and to secrete a major number of extra-cellular matrix components (ECM). Such modified fibroblasts are known as cancer-associated fibroblasts, CAFs. About 80% of stromal fibroblasts in breast carcinomas are thought to acquire this activated phenotype (78). CAFs, probably, also promote tumour progression through specific communications with cancer cells. For example, CAFs facilitate the invasiveness of otherwise non-invasive cancer cells when co-injected into mice (79). CAFs promote neoplastic development through the secretion of molecules soluble as pro-angiogenic factors, metalloproteinases (MMPs), cytokines, chemokines and growth factors. SDF-1 (CXCL12) represents a molecule widely involved in the crosstalk between CAF and cancer cells, as it increases the proliferation, migration and invasion of cancer cells, as well as induces an increase in angiogenesis by recruiting endothelial progenitor cells in carcinomas (80). CAFs also promote stem cell proliferation $CD44^{+}/CD24^{-}$ in mammospheres in an SDF-1-dependent manner, improving tumorigenicity in mice (75). Moreover, the presence of CAFs is an effective predictor of tumor recurrence in colorectal cancer patients and has been highlighted as a significant prognostic factor in a number of tumor types (81). CAFs can originate from Mesenchymal stem cells trans-differentiation. In the

tumor microenvironment, the contact with cancer cells can induce a mesenchymal-mesenchymal transition of MSCs in cancer-associated fibroblasts (CAFs); this trans-differentiation results in the acquisition of specific markers such as FAP (Fibroblastic-Activation-Protein) and ACTA2 coding for aSMA (α-smooth muscle actin). Therefore, tumor cells can favor the trans-differentiation into CAF through an "in vivo education" of normal fibroblasts (82); indeed, cancer cells, through the release of pro-inflammatory interleukins, such as IL-1, induce the expression of pro genes -inflammatory and pro-angiogenic characterizing CAFs. These, in turn, can attract neutrophils and macrophages, cells capable of supporting the process of tumor-associated neo-angiogenesis (83) (Figure 6). Higher expression of αSMA-positive fibroblasts has been strongly linked to lower overall survival in breast and colon cancer (84). In addition, it was demonstrated that the α-SMA expression significantly correlates with the development of metastatic disease (85). FAP has traditionally been associated with tissue repair, fibrosis and extracellular matrix degradation by fibroblasts due to its dipeptidyl peptidase and collagenase activity (86). FAP is one of the most strongly expressed genes in the tumor stroma and is upregulated in over 90% of epithelial carcinomas. Due to its high expression in the tumor stroma, numerous studies have used FAP as a marker of activated cancer-associated fibroblasts (87-88)

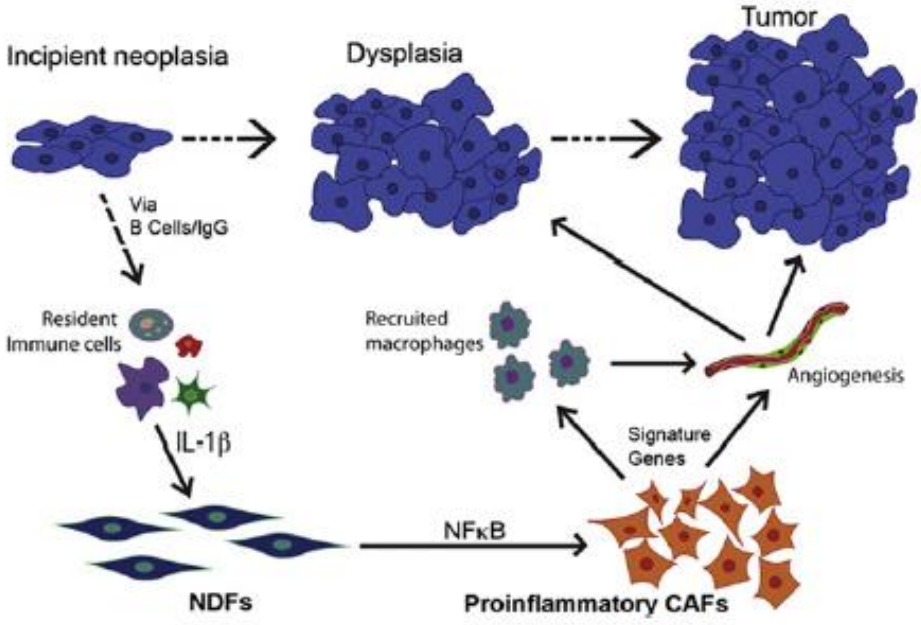

Figure 6. CAFs in tumoral progression (Erez, Truitt, Olson, Arron, & Hanahan, 2010)**.**

Senescence is a cellular process that can function in opposite directions. It is a potential mechanism for a cell to avoid malignant transformation. However, senescence can also promote cancer development by altering the cellular microenvironment through a senescence-associated secretory phenotype (SASP). There are three types of cellular stress, such as activation of oncogenes, loss of tumor suppressor genes, and chemo/radiotherapy, that can induce cell senescence. Oncogene-induced senescence can be associated with replicative senescence. Early-stage senescence may protect cell from transformation, while prolonged senescence often promotes cancer development (89). The significance of senescence during breast cancer progression is not well established. Alteration of the senescence pathway through p53/ARF or p16/Rb may be important in breast cancer progression (90). The cyclin-dependent kinase inhibitor, p16, has become an important player in ageing and age-related disease. Biochemically, p16 inactivates CDK4 and CDK6, which maintains pRB in its active, hypophosphorylated form and consequently blocks cell cycle progression in G1 (91). p16 expression can be upregulated by a wide variety of stresses (92); it may be involved in many forms of senescence and is considered one of the main senescent biomarkers. It has been shown that senescent stromal cells in the TME promote tumor aggressiveness and are a primary cause of therapy resistance. Accumulating evidence suggests that senescence fibroblasts promote tumorigenesis and tumor growth by expressing a pro-tumorigenic factor known as the senescence-associated secretory phenotype (SASP)(93). In addition, senescent cells can promote epithelial-to-mesenchymal transition (EMT), a crucial step in tumor cell metastasis. It has been shown that treatment of human breast cancer cell lines with conditioned media from senescence fibroblasts resulted in decreased expression of cytokeratin and E-cadherin, hallmarks of EMT (94).

Lamin B1 is a nuclear intermediate filament protein, located within the inner surface of the nuclear envelope and is encoded by the *LMNB1* gene. Lamin B1 plays a key role in nuclear stability, DNA replication, gene transcription, cell proliferation, ageing, and in response to oxidative stress (95). Interestingly, the degradation of Lamin B1 is considered a component of nuclear envelope remodelling, that occurs as a cell undergoes senescence and is now utilized as an

established biomarker for identifying senescent cells in vitro (96). Recent work has focused on identifying and elucidating the mechanisms that drive the emergence of cancer-initiating cells or cancer stem cells (CSCs), which appear to be responsible for forming distant metastasis (97). Emerging data suggest that the tumor microenvironment can influence CSCs prevalence. Intriguingly, chemokines secreted by senescent cells have been shown to select for CSCs. IL6, one of the most highly expressed SASP factors, can play an important role in regulating breast CSC self-renewal (98). Similarly, analyses of breast CAFs recently revealed that expression of chemokine (C-C motif) ligand 2 (CCL2) can stimulate CSC properties, including sphere-forming capacity and self-renewal (99). Targeting senescent fibroblasts may be a novel and efficient cancer therapy.

2. Aims of the study

Epidemiological studies report that patients with type 2 diabetes (T2D) show an increased risk of developing several types of cancer, including breast cancer (100). Associations between T2D and breast cancer have been intensively studied, particularly regarding diabetes and the risk and prognosis of breast cancer (16). Diabetes is associated with a 14% to 25% increased risk of breast cancer, with a 37% to 61% elevated hazard of all-cause mortality in breast cancer patients. (101). The tumor microenvironment plays an important role in neoplastic development (51). Adipose tissue represents an important component of the tumor microenvironment, especially in breast cancer and actively intervenes in the association between diabetes and cancer (54). Hyperglycemia represents the main metabolic alteration that characterizes T2D and is associated with a more aggressive cancerous phenotype in breast cancer patients. Mammary Adipose tissue (MAT) responds to metabolic, inflammatory and tumoral stimuli by releasing various molecules to sustain breast cancer cells proliferation, migration, invasiveness and drug resistance (57,58,59). MAT is rich in Mesenchymal Stem Cells (MSCs), which may support tumour phenotype by either acting as energy reservoirs for cancer cells or through the secretion of signaling molecules (66). In turn, cancer cells, following metabolic alterations like hyperglycemia, may modify the surrounding-MSCs phenotype for their own advantage. Thus, MSCs and cancer cells establish a dangerous duo. In this *scenario*, diabetes-associated hyperglycemia may affect on both cancer and surrounding stromal cells, including MSCs.

Thus, this PhD work aims to investigate the impact of glucose on the bi-directional communication between breast cancer cells and mesenchymal stem cells and the effect of glucose-modulated MSCs onto MCF7 breast cancer cells progression and aggressiveness.

3. Material and Methods

3.1 Isolation of MSCs from Mammary Adipose Tissue

MAT biopsies were obtained from healthy women (N = 20) undergoing surgical mammary reduction, free of neoplastic, metabolic or endocrine diseases. The biopsies were processed under a laminar flow hood. Once washed to remove traces of blood with DMEM culture medium (Dulbecco's Modified Essenzial Medium) F12 (1: 1) supplemented with 10% fetal bovine serum (FBS), 2mM L-Glutammine, 100 U/ml penicillin, 100 IU/ml streptomycin and 1.5 μg/ml amphotericin, biopsies were mechanically processed using sterile scissors, then they have been digested with 1mg/ml collagenase for 45 minutes under agitating in a water bath at 37°C . The tissue digested has been filtered with a nylon filter (250 μm). After about 10min, phase separation was obtained, a denser yellow upper phase and a more liquid lower. It was possible to isolate mature adipocytes from the upper phase and cells of the vasculo-stromal fraction (SVF) containing the MSCs from the lower phase. SVF cells were centrifuged for 5 minutes at 1300 rpm. After removing the supernatant, the pellet was resuspended in DMEM-F12 10% FBS and seeded in a 25 cm2 flask.

3.2 Cell cultures

MCF-7 breast cancer cells were isolated in 1970 from a breast tumor of a 69-year-old Caucasian American woman. MCF-7 is the acronym of the Michigan Cancer Foundation -7, Detroit (USA) institute, where the cell line has been cultivated and linearized in 1973 by Herbert Soule and his collaborators (Soule, HD; Vazquez J; Long A; Albert S; Brennan M. (1973). "A human cell line from a pleural effusion derived from a breast carcinoma". Journal of the National Cancer Institute.). These breast cancer cells are estrogen and progesterone receptors positive (ER^+, PR^+). MSCs were cultured in DMEM-F12 (1:1). MCF-7s were cultured in 100mm diameter plates in DMEM 25 Mm glucose. Both media were supplemented with 10%FBS, 2 mM L-Glutamine (SIGMA), penicillin (100 U / ml), streptomycin (50 μg / ml) and amphotericin B (1.5 μg / ml) (SIGMA). Cultures were maintained in

a humidified atmosphere of 95% air and 5% CO2 at 37 ◦C. The cells reached the required confluence have been detached from the plate using a solution of Trypsin (0.3%), Glucose (0.1%) and EGTA (2 mM) dissolved in PBS pH 7.3 (13.7 mM KCl, 1.47 mM KH2PO4, 8.06 mM Na2HPO4, H2O), centrifuged in tubes of 15ml for 5 'at 1300 rpm and finally resuspended in fresh culture medium and plated at a specific concentration.

3.3 2D-cultures

MSCs (2.5×10^4 cells) were seeded in the bottom chamber of a transwell-6 culture system, while MCF7 were plated (3.5×10^4 cells) in the upper chamber, specifically, permeable support, which had a membrane of Polyethene terephthalate (PET) with 0.4 μm pore size. Cells co-cultured were exposed to25mM glucose (High Glucose; HG), resembling hyperglicemia in humans, or to 5.5mM glucose (Low Glucose; LG). In parallel, BC cells and MSCs were monocultured in HG or LG medium. After 72 hrs, cells were harvested for RNA extraction or cytofluorimetric analysis.

3.4 3D-cultures

Spheroid formation: MCF7 (4×10^5) were plated in ultra-low attachment 100mmx20mm (CORNING, NY, USA) with or without MSCs (1×10^5) in HG or LG medium supplemented with 5% FBS. After 72 hrs, spheroids were mechanically disaggregated to obtain cells for cytofluorimetric analysis or zebrafish injection.

Mammosphere-forming assay: MCF7 cells were plated in ultra-low attachment 96-wells (Corning, NY, USA) with or without MSCs (ratio 4:1) in HG or LG medium supplemented with 5% MammoCult™ Proliferation Supplement (STEMCELL Technologies, BC, Canada). After 10 days, mammosphere number was quantified (number of formed spheres/number of wells containing cells × 100). In parallel, mammosphere diameter was measured by a software associated to the Olympus DP20 microscope digital camera system.

3.5 Cytofluorimetric Analysis

Quantification of $CD44^{high}/CD24^{low}$ BC cell sub-population: MCF7 were harvested in 15 ml tubes (FALCON) and centrifuged for 5 minutes at 1300 rpm. Then, the pellet was resuspended in 1 ml of cold PBS 1X. After centrifuge for 5 minutes at 350 rcf at 4°C, the cells were incubated for 30 minutes at 4°C with APC-anti-CD44 and PE-anti-CD24 (BD Biosciences, USA) as well as dye/isotype control matched antibodies. The cells were centrifuged at 350 rfc for 5 minutes at 4°C, washed with 1ml of PBS1X and resuspended in 300microliters of PBS1X. Samples were processed using a BD LSR Fortessa or using a FACSCalibur (BD Biosciences) and analyzed by using BD FACS Diva software or Cell Quest software.

Protein levels in 3D-cultures: Spheroids were disaggregated and cell membranes were permeabilizated by using the Cytofix/Cytoperm kit (BD Biosciences) before incubation (4°C, 30 min) with specific or isotype control antibodies. Positivity to cytokeratin (FITC-anti-cytokeratin; cat.130-112-743, Miltenyi Biotec) was used to discriminate MCF7 from MSCs. PE-anti-OCT4 was from Cell Signaling (cat. 2750S, Danvers, MA, USA), anti-αSMA was from Dako (cat. M0851, Carpinteria, CA, USA), secondary anti-mouse PE antibody used to conjugate anti-αSMA antibody was from Miltenyi Biotec (cat.130-095-908), APC-anti-FAP was from R&D System (cat. FAB3715A), APC-anti-p16 was from Miltenyi Biotec (cat. 130-116-138). Samples were processed using a BD LSR Fortessa or a FACSCalibur (BD Biosciences) and analyzed using BD FACS Diva software or Cell Quest software. 104 events for each sample were acquired in all analyses.

3.6 RNA Isolation and Analysis

MSCs and MCF7 were collected from 2D co-cultures, centrifuged and the pellets obtained were lysated using TRIzol solution total. (Life Technologies, Carlsbad, CA, USA). The lysates were incubated for 5 minutes at room temperature to permit complete dissociation of the nucleoprotein complex. Next it was added 0.2 mL of chloroform per 1 mL of TRIzol Reagent. The samples were incubated for 2-3 minutes at room temperature and centrifuged at 12,000 rcf for 15 minutes at 4°C.

Chloroform permits to separate the mixture into a lower red phenol-chloroform phase, interphase, and a colourless upper aqueous phase. RNA remains exclusively in the acqueous phase. Then, the aqueous phase was removed and placed into a new tube to proceed to RNA isolation. 0.5 mL of 100% isopropanol per 1 mL of TRIzol Reagnt has been added to the aqueous phase, that has been incubated at room temperature for 10 minutes. After incubation and centrifugation at 12,000 rcf for 10 minutes at 4°C, supernatant has been removed from the tube, leaving only the RNA pellet. The pellet has been washed with 1 mL of 75% ethanol per 1 mL of TRIzol Reagent, then vortexed and centrifuged at 7500 rcf for 5 minutes at 4°C. The supernatant has been discarded and RNA pellet dryed has been resuspended in H_2O RNasi-free. RNA samples were quantified by measuring the absorbance at 260 nm and 280 nm (NanoDrop spectrophotometer, Life Technologies).

3.7 RT-PCR

RNA samples were reverse-transcribed using SuperScript III Reverse Transcriptase with oligo dT primers (cat. 18080-044, Life Technologies). To each sample of RNA (1000 ng diluted in water in a final volume of 11µL) have been added: dNTP Mix (10 mM; 1µL), oligo dT primers (1µL), RTBuffer 5x (4µL), DTT (2µL), RNase OUT (1µL) and Superscript III Reverse Transcriptase (1µL). The samples were placed in a thermal cycler (Biorad T100) and using the following cycling condition: 25 ° C for 5 minutes, 50 ° C for 60 minutes and 70 ° C for 15 minutes. To check the amplifiable template RNA/cDNA, RT-PCR amplification of housekeeping gene was performed. Amplification reactions were set up using AmpliTaq Gold (cat. N8080247, Life Technologies), and specific primers of housekeeping gene were designed by Oligo 4.0.
(*PPIA FW 5'TACGGGTCCTGGCATCTTGT3'; PPIA RW 5'GGTGATCTTCTTGCTGGTCT3'*).
PCR products were analyzed by electrophoresis on agarose gel.

3.8 Quantitative Real-Time RT-PCR (qPCR)

cDNA from cells was then used as a template for quantitative real-time PCR assays. In detail, for each sample, reactions were performed in triplicates using iQ SYBR Green Supermix on an iCycler real-time detection system (Bio-Rad Laboratories), by using the following cycling condition and reaction protocol. Cycling condition: 10 min at 95° C for 1 cycle, and 15 s at 95° C and 1 min at 60° C repeated for 40 cycles. Reaction protocol: cDNA (1000ng/µl), forward and reverse PCR primers (10µM, 0.4 µl), iQ SYBR Green Supermix 1X (Bio-rad laboratories) (5 µl) in a final volume of 10 µL. Relative quantification of gene expression was measured by using $2^{-\Delta\Delta Ct}$ method. Expression levels were normalized for the reference sample using peptidylprolyl Isomerase A (PPIA) as housekeeping gene. Primer sequences were as follow:

OCT4 F:	*5'-TCAGCCACATCGCCCAGCA- 3'*
OCT4 R:	*5'-AGGGAAAGGGACCGAGGAG-3'*
SOX2 F:	*5'-CAACCAGAAAAACAGCCC G-3'*
SOX2 R:	*5'-CAGCCGCTTAGCCTCGTC-3'*
NANOG F:	*5'-CCTGAAGAAAACTATCCATCC-3'*
NANOG R:	*5'-GTTCTGGTCTTCTGTTTCTTG-3'*
ACTA2 F:	*5'- AGAACATGGCATCATCACCA-3'*
ACTA2 R:	*5'-GAGTCATTTTCTCCCGGTTG- 3'*
CDKN2A F:	*5'-CGGAAGGTCCCTCAGACATC-3'*
CDKN2A R:	*5'-AAACTACGAAAGCGGGGTG- 3'*
LMNB1 F:	*5'-GCCCAGATCAAGCTTCGAGA-3'*
LMNB1 R	*5'-GCTTCCAACTGGGCAATCTG- 3'*

3.9 In Vivo Zebrafish Model

Cell culture and labeling: MCF7 and MSCs from 3 different donors were labeled with red cell trackers CM-DiI (cat. C7000, Thermo Fisher Scientific, Waltham, MA, USA) and BioTraker 400 Blu (cat. SCT109, Millipore, MA, USA), respectively—according to manufacturer's instructions—before spheroid formation. After 72 h, spheroids were trypsinized, washed and resuspended in PBS/EDTA for zebrafish xenotransplantation. Zebrafish husbandry and xenotransplantation: Animal experiments were in accordance with the European Council Directive 2010/63/EU and approved by the Biogem s.c.ar.l. internal ethics committee. Animal care was in accordance with institution guidelines.Tg(fli1:EGFP) zebrafish line, with green fluorescent vessels was raised, maintained and paired under standard conditions. Zebrafish eggs were obtained from natural spawning and maintained at 28 ◦C for 48 h in E3 medium (5 mM NaCl, 0.17 mM KCl, 0.33 mM CaCl2, 0.33 mM MgSO4). Two days post-fertilization (dpf), embryos were dechorionated and anesthetized with 0.04% of tricaine (Sigma Aldrich, St. Louis, MO, USA) before cell microinjection. Approximately 100–200 cells/embryo were injected in the perivitelline space of each embryo using a pneumatic PicoPump PV830 injector (World Precision Instruments, Sarasota, FL, USA) equipped with an injection borosilicate glass needle (Sutter instruments, Novato, CA, USA). Following transplantation (0 h post injection), larvae with correct engraftment in the yolk sac were selected under Leica M205 FA fluorescence stereo microscope (Leica, Mycrosystems, Wetzlar, Germany) for further analysis and kept at 34 ◦C for 72 h. Embryos injected with same volume of PBS/EDTA were defined as control embryos.

Imaging: Zebrafish larvae were anesthetized and evaluated at 0 and 72 h post-injection by fluorescence stereo microscope. Different filters were selected for fluorescence imaging and captured with a Leica DFC450 C camera. Images of embryos at different stages of each experimental group were analyzed with ImageJ software (National Institutes of Health,Rockville, MD, USA).

3.10 Mammospheres viability assay

The viability of the mammospheres has been measured by reading the luminescence, by using CellTiter-Glo3D Cell Viability Assay (Promega, USA). This assay determines the number of viable cells in 3D cell culture based on quantitation of cellular ATP, which is a marker of metabolically active cells. CellTiter-Glo 3D Reagent, the plate and its contents have been equilibrated to room temperature for 30 minutes. After equilibration, CellTiter-Glo 3D Reagent is directly added to each well (100µl/well). Next, the plates were placed on a shaker for 10 minutes and equilibrated at room temperature for 15 minutes to stabilize the luminescence signal. The luminescence was measured in Corning 96 well white/clear plates and recorded by integration time of 0.25-1 second per well, by using Glomax Discover Microplate Reader (Promega, Madison, WI, USA). The data were expressed as mean ± SD of viable cells relative to the control. Images of mammospheres were taken by the Olympus DP20 microscope digital camera system (Olympus Corporation, Tokyo, Japan).

3.11 Statistical Analysis

Statistical analyses were performed using GraphPad Prism 7.0 software (GraphPad Software Inc., La Jolla, CA, USA). Kruskal Wallis and Friedman tests followed by Dunn's correction were applied for multiple comparisons; Wilcoxon and Mann–Whitney U tests were used for pairwise comparisons, as indicated in figure/table legends. Percentages were compared by chi-square with Fisher's exact test. p-value < 0.05 was considered statistically significant. Sample sizes were determined based on the means and variations of previous pilot experiments. Hence, no statistical power analysis was used. Replicates for all the experiments were from different samples isolated from different human specimens, as indicated in figure legends.

3.12 Single-cell RNA sequencing

Cell nuclei have been isolated from cell samples for single-cell RNA sequencing by using the Isolation of Nuclei from single cell suspensions protocol (10x Genomics). At first, cells were lysed adding a Lysis Buffer; then nuclei were washed and resuspended, adding the appropriate volume of Nuclei Wash and Resuspension Buffer. Nuclei concentration was determined using a Countess II FL Automated Cell Counter. Next, Single-cell transcriptional profiling was performed using the 10x Chromium platform and libraries were generated using the Chromium Next GEM Single Cell 3' kit. Chromium Next GEM Single 3' protocol consists of 3 steps, providing for GEM Generation and Barcoding; Post GEM-RT Cleanup and cDNA Amplification and 3' Gene Expression Library Construction. An Agilent Bioanalyzer High Sensitivity chip has been used post-library construction to check the quality and determine the quantification of libraries. The 3' Gene Expression libraries have been pooled for ILLUMINA sequencing, considering the differences in cell number and per-cell read depth requirements between each library. Bioinformatical analyses with the Seurat software suite have followed single-cell sequencing. To remove low-quality cells and doublets, cells with very high mitochondrial gene percentage were filtered out. Thus, ~10000 cells were analyzed with a median of 1155 genes per cell and a median of 2007 UMI counts per cell, except for MSC non-naïve sample (median genes per cell were low, with high mitochondrial gene percentage). It was performed unsupervised clustering of cell samples to analyze by using Seurat. R-based ShinyApp platform was used to analyze gene expression, cell number, mt-transcription and make graphs.

Gene enrichment analysis was performed by using different databases: Gene ontology (GO) to identify biological process and protein class; ProteomicsDB 2021, CCLE Proteomics 2020, Cell Marker Augmented 2021 to identify Cell Types and Transcription Factors PPIs dataset to identify expression of TF target genes and interactors.

Pathway analysis of DEGs (Differential gene expression) was performed using the WIKI Pathway 2021 Human and the KEGG Pathway Human 2021 databases. Tables, bar chart plots and graphs were obtained by using the Appyter platform.

4. Results

4.1 Impact of glucose on the dialogue between MSCs and MCF7 BC cells in 2D culture

Stem Cell sub-population (CSC) are tumor-initiating cells, able to promote cancer progression, metastasis, recurrence and drug resistance. Adipose tumor microenvironment influences the prevalence of CSC in BC. Thus, the effect of mammary adipose-derived MSCs and the possible role of glucose onto cancer cell stemness phenotype has been evaluated. To this aim, MSCs and MCF7 cells were co-cultured in 2D system, permitting a bi-directional communication between cells, even in absence of physical interactions. Cells were co-cultured by exposing the system to high glucose (HG; 25 mM) or low glucose (LG; 5.5 mM), resembling hyperglycemia or normoglycemia in humans, respectively. After 72 hours, cancer stem-like $CD44^{high}/CD24^{low}$ sub-population was quantified in MCF7 by cytofluorimetric analysis. As shown in Figure 7, the percentage of $CD44^{high}/CD24^{low}$ cells was 15-fold significantly increased when MCF7 cells were co-cultured with MSCs in HG, while not in LG, suggesting that glucose promotes the ability of MSCs to induce the acquisition of stem-like phenotype in cancer cells.

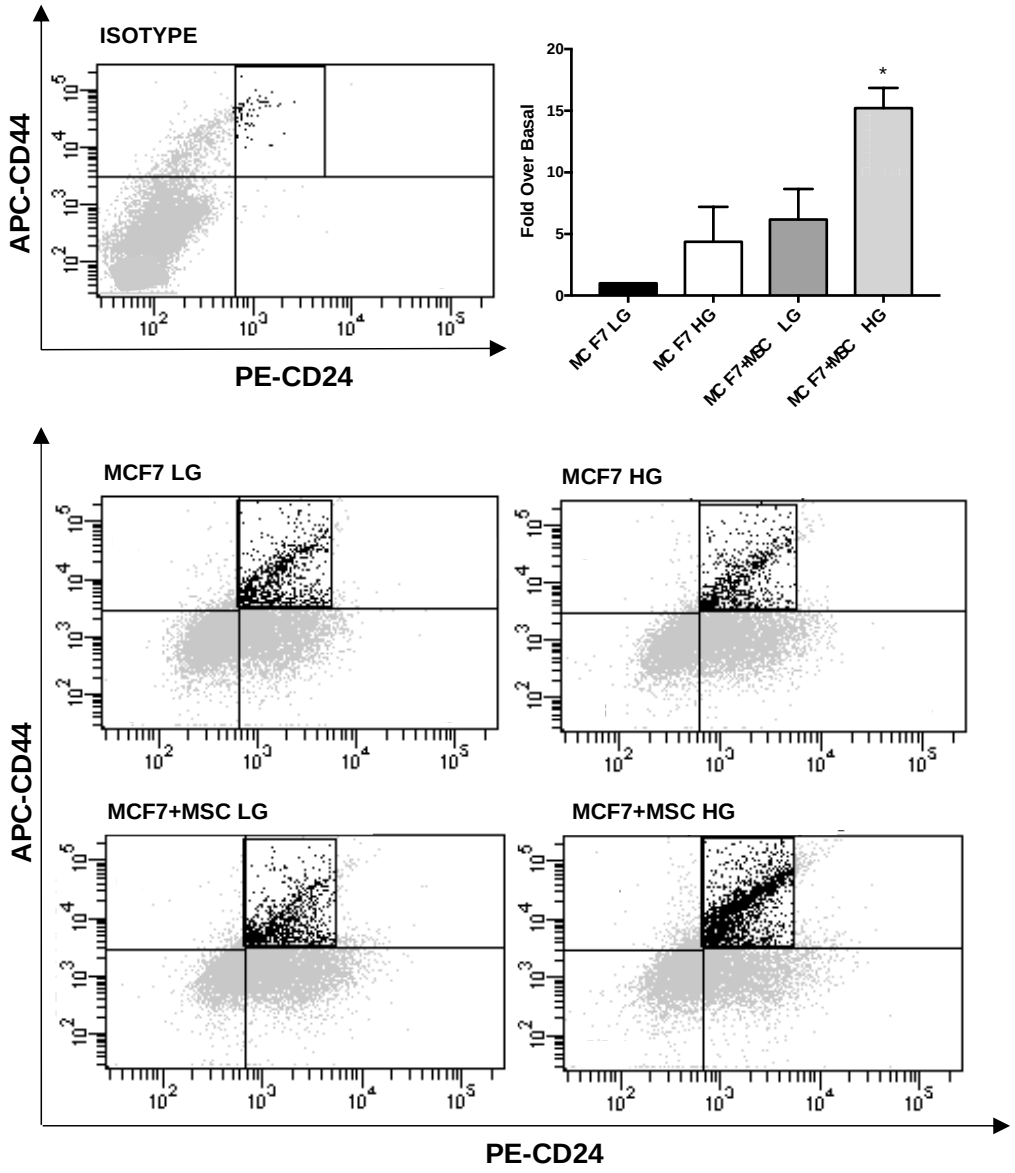

Figure 7. Quantification of CD44^{high}/CD24^{low} subpopulation in MCF7 co-cultured with MSCs. MCF7 were co-cultured -and not- with MSCs in high glucose (25mM; HG) or in low glucose (5.5mM; LG) medium for 72 hrs. After 72 hrs, CD44^{high}/CD24^{low} stem cell subpopulation was identified in monocultured (MCF7 LG/HG) and co-cultured (MCF7+MSC LG/HG) MCF7 by cytofluorimetric analysis. Representative dot plots show MCF7 stained with APC- anti-CD44 and PE-anti-CD24 as well as dye/isotype-matched antibodies. In the graph, the population percentage was reported as fold over basal (MCF7 LG) and showed CD44^{high}/CD24^{low} cell subpopulation as mean ±SD of 4 independent experiments. Data were analyzed using the non-parametric Friedman test followed by Dunn's correction for multiple comparisons. *denote statistically significant values compared with MCF7LG (*adjp<0.05).

To further investigate such aspect, stemness markers OCT4, SOX2 and NANOG were measured in MCF7 cells co-cultured with MSCs in HG or LG. As shown in Figure 8a, *SOX2* and *NANOG* mRNA levels remained unaltered in MCF7 co-cultured with MSCs, independently of glucose levels. Interestingly, only in HG, *OCT4* mRNA levels were significantly increased - compared to relative mono-cultures - in MCF7 co-cultured with MSCs ($pval<0.05$) (Figure 8a), thus confirming the glucose-modulated impact of MSCs to promote stemness phenotype in MCF7. To better define the bi-directional communication between cancer and adipose-derived MSCs, the impact of glucose and MCF7 onto multipotency of MSCs was investigated in the same system. Thus, upon 2D-culture in HG or LG, mRNA levels of *OCT4*, *SOX2* and *NANOG* were measured in MSCs. Notably, it was observed that co-cultures with MCF7 significantly reduced mRNA levels of *OCT4* (about 30% reduction) and *SOX2* (about 80% reduction) in MSCs in HG while not in LG (Figure 8b; $pval<0.05$). At variance, *NANOG* expression was not changed in MSC co-cultured with MCF7 in HG or LG (figure 8b). Therefore, in high glucose, MCF7 induce the loss of multipotency of mesenchymal stem cells.

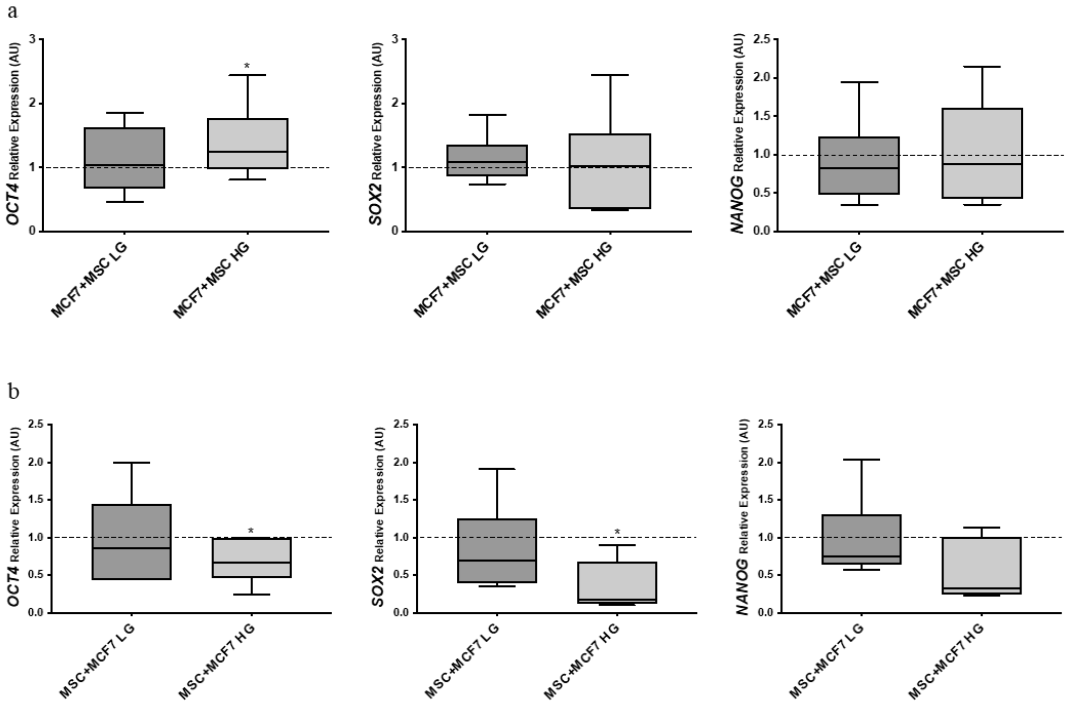

Figure 8. Effect of glucose onto MCF7 and MSC stemness in 2D culture. 8a) MCF7 were co-cultured -and not- with MAT-MSCs in high glucose (25mM; HG) or in low glucose (5.5mM; LG) medium for 72 hrs. After 72 hrs, mRNA expression levels of stemness (*OCT4, SOX* and *NANOG*) were determined by qPCR. Data were normalized on *PPIA* gene as an internal standard. Results were represented as box-plot of 7-15 indipendent triplicate expertiments showing mRNA levels of *OCT4, SOX2* and *NANOG* in MCF7+MSC LG/HG as relative expression ($2^{-\Delta\Delta Ct}$) compared to that in mono-cultured cell (MCF7 LG/HG). Data analyzed using non-parametric Mann-Whitney test. *denote statistically significant values (*pval<0.05). **8b)** MSCs were co-cultured—and not—with MCF7 standard/high glucose (25mM; HG) or in low glucose (5.5mM; LG) medium for 72 hrs. After 72 hrs, mRNA expression levels of stemness (*OCT4, SOX* and *NANOG*) were determined by qPCR. Data were normalized on *PPIA* gene as an internal standard. Results were represented as box-plot of 7-9 independent triplicate experiments showing mRNA levels of *OCT4, SOX2* and *NANOG* in MSC + MCF7LG/HG as relative expression ($2^{-\Delta\Delta Ct}$) compared to that in mono-cultured cells (MSC LG/HG). Data were analyzed using the non-parametric Mann-Whitney test. *denote statistically significant values (*pval<0.05).

Overall, these results demonstrated that glucose influences the cross-talk between breast cancer and adipose-derived cells. Specifically, it promoted phenotypic changes in both cell types, leading to the acquisition of stem-like features in MCF7 (increased level of stemness gene expression, *OCT4* and increased percentage of $CD44^+/CD24^-$ BC subpopulation) paralleled by the loss of multipotency in MSCs (reduction of gene expression levels of *OCT4* and *SOX2*).

4.2 Impact of glucose on the dialogue between MSCs and MCF7 BC cells in 3D culture

Because of its ability to mimic tissue structure and function, 3D culture system has become essential for tumor research. It allows the study of the cellular changes and interactions during tumoral progression, representing a more physiological and avant-garde system than 2D culture. Therefore, such approach was adopted to investigate the dialogue between MSCs and MCF7 better and to define how glucose may interfere with this communication. Thus, MCF7 were grown in anchorage-independent manner by plating them in ultra-low-attachment plates in presence and absence of MSCs in HG or LG. After 72 hours, obtained spheroids were mechanically disaggregated and subjected to flow cytometric analysis to measure OCT4 protein expression as stemness/multipotency marker in both cancer and adipose-derived cells. In keeping with gene expression data (Figure 8), spheroids-derived MCF7 displayed a 4.3-fold increase of OCT4 protein (adjp<0.001) paralleled by a 50% significant reduction of OCT4 protein (adjp<0.05) in spheroid-derived MSCs, both in HG while not in LG (Figure 9). These data confirmed that glucose promotes the reciprocal impact of BC cells and MSCs, determining the acquisition of a stem phenotype in MCF7 and the loss of multipotency in MSCs.

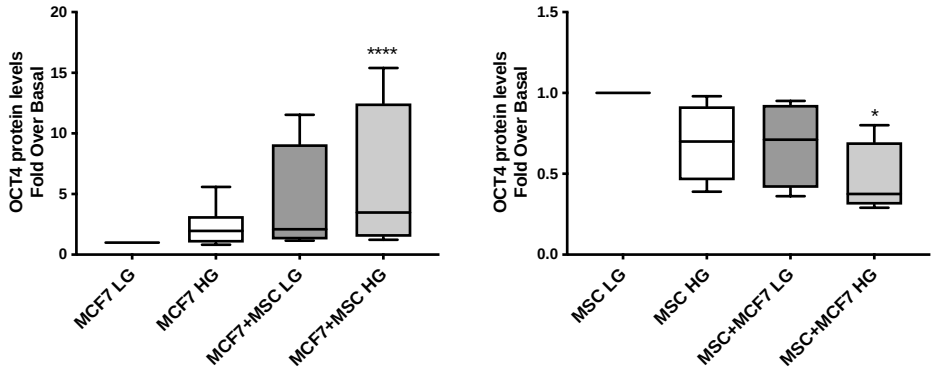

Figure 9. Effect of glucose on MSCs and MCF7 stemness in 3D-spheroids. 3D cultures were set up using MCF7 and MSCs (ratio 4:1) in LG or HG concentrations. After 72 hrs, spheroids were mechanically disaggregated, cells were stained FITC-anti-OCT4 and dye/isotype-matched antibodies for cytofluorimetric analysis. Results were reported as box plot of 4-9 independent experiments showing protein levels of OCT4 in MCF7 and in MSCs as fold over basal (MCF7 LG/MSC LG). Data were analyzed using non-parametric Friedman test followed by Dunn's correction for multiple comparisons. *denote statistically significant values compared with MCF7 LG or MSC LG(*adjp<0.05; ****adjp<0.001).

As a consequence of phenotypic changes induced by MCF7 in MSCs, the potential acquisition of senescent/fibrotic features was investigated. Thus, myofibroblast trans-differentiation (a-SMA and FAP) and senescent markers (p16 ^{INK4a} and LAMIN B1) were measured in MSCs both at mRNA and protein levels in 2D and 3D systems. Interestingly, a significant increase of a-SMA (adjp<0.05), FAP (adjp<0.01) and p16^{INK4a} (adjp<0.05) proteins were observed in spheroid-derived MSCs in HG while not in LG (Figure 10a). In line with this, only in HG, mRNA levels of *ACTA2* (encoding a-SMA) (adjp<0.001), *CDKN2A* (encoding p16 ^{INK4a}) (adjp<0.01), and *LMNB1* (encoding LAMIN B1) (adjp<0.01) were significantly modified in MSCs co-cultured with MCF7 than in monocultured cells (Figure 10b). Such results highlighted that glucose promotes the acquisition of fibrotic and senescent-like features in MSCs co-cultured with MCF7.

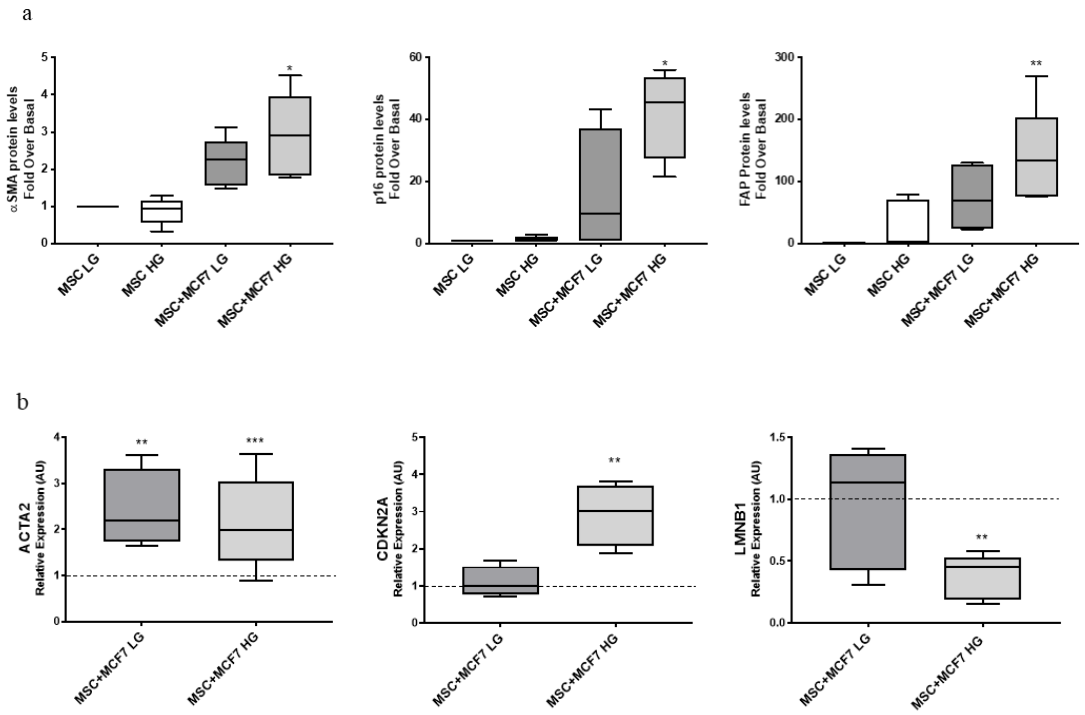

Figure 10. Effect of glucose on MSCs phenotype in 3D and 2D cultures. 10a) 3D cultures were set up using MCF7 and MSCs (ratio 4:1) in LG or HG concentrations. After 72 hrs, spheroids were mechanically disaggregated, and MSCs were stained PE-anti-aSMA, APC-anti-FAP and APC-anti-p16, as well as dye/isotype-matched antibodies for cytofluorimetric analysis. Results were reported as box plot of 4-9 independent experiments showing protein levels of aSMA, FAP and p16 and in MSCs as fold-over basal (MSC LG). Data were analyzed using non-parametric Friedman test followed by Dunn's correction for multiple comparisons. *denote statistically significant values compared with MSC LG(*ADJP<0.05; **adjp<0.001). **10b)** 2D cultures were established co-culturing MSCs with and not MCF7 in HG or LG. After 72 hrs, mRNA expression levels of fibrotic (ACTA2) and senescent markers (CDKN2A and LMNB1) were determined by qPCR. Data were normalized on PPIA gene as internal standard. Results were represented as-box plot- of 7-9 independent triplicate experiments showing mRNA levels of *ACTA2*, *CDKN2A* and *LMNB1* in MSCs co-cultured with MCF7 as relative expression ($2^{-\Delta\Delta Ct}$) compared to that in monocultured MSCs (LG/HG). Data were analyzed using the non-parametric Mann-Whitney test. *denote statistically significant values compared with monocultured MSC (**adjp<0.001, ***adjp<0.0001).

4.3 *In vivo* model to define the glucose-modulated MSC effect onto MCF7

Glucose intervenes in the dialogue between cancer and adipose-derived cells sustaining the acquisition of a stem-like phenotype in MCF7 and a potential trans-differentiation of MSC toward senescent CAFs. The latter displays a known pro-tumorigenic function, promoting cancer cell growth, angiogenesis, and invasion. Thus, a glucose-modulated pro-metastatic effect of MSCs on MCF7 was investigated by establishing a zebrafish xenograft model. To this aim, spheroids-derived cells were engrafted in 2 days old zebrafish embryos (Figure 11a).

Immediately after injection, cells were localized in the yolk sac (figure 11a, red spot). At 72 hours post-injection, cells were able to migrate in head and tail regions (Figure 11b, with arrows). Mono-cultured MCF7 in LG and HG showed a similar dissemination rate (figure 11b). Interestingly, in LG, the percentage of xenografts with invasive MCF7+MSCs was significantly reduced compared to MCF7 mono-cultured, and most zebrafish displayed a clear localized tumour mass (figure 11b, big white arrow). At variance, in HG the percentage of xenografts with invasive MCF7+MSC was significantly higher compared to MCF7 monocultured (Figure 11b). Thus, the injection of spheroids MSC+MCF7-derived cells, in HG, led to higher tumor invasiveness.

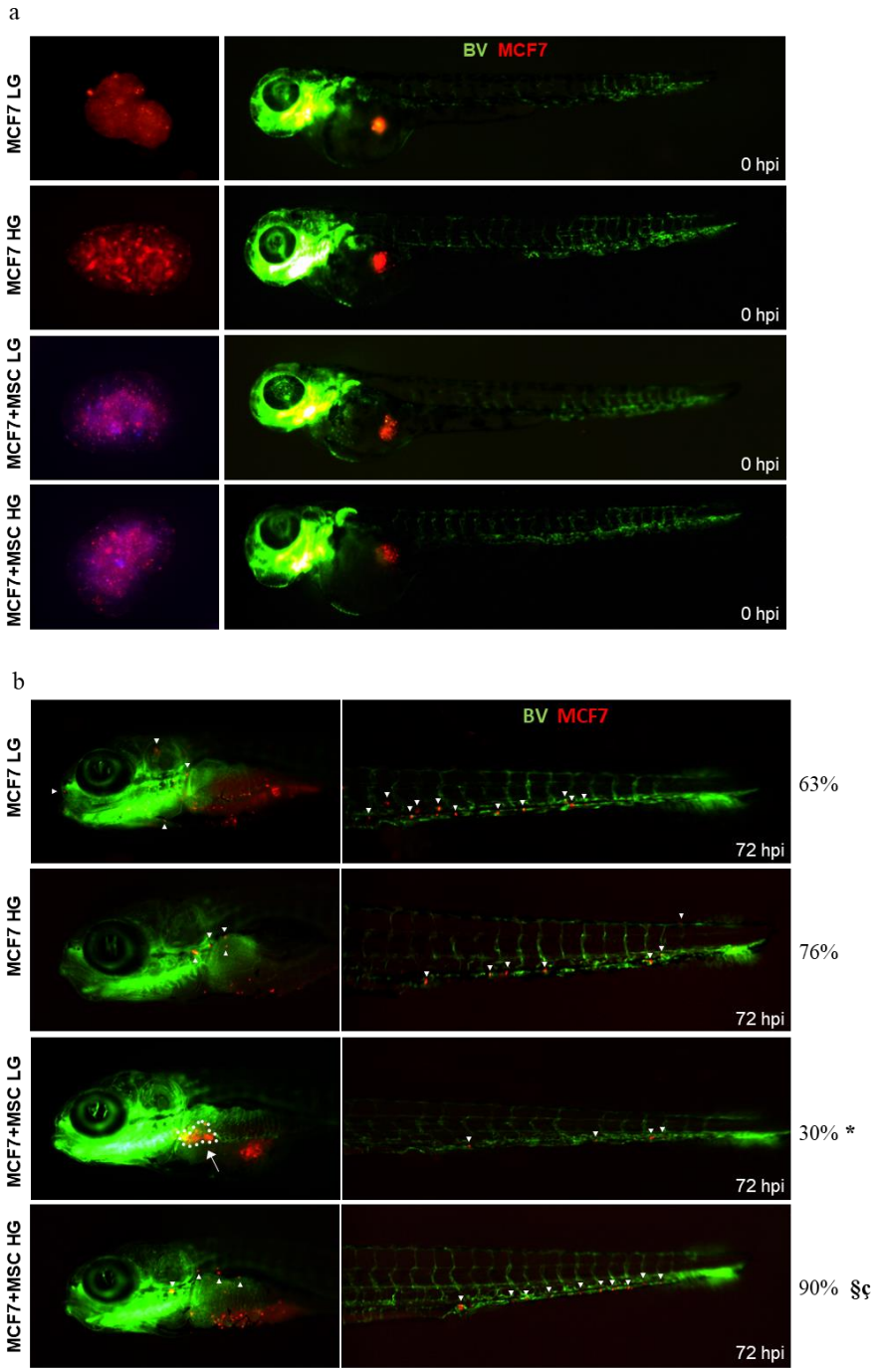

Figure 11. Effect of glucose on MCF7+MSCs organoids in xenograft zebrafish models. MCF7 (labelled with red dye), cultured in spheroids alone or with MSCs (labelled with blue dye) in LG or HG, were injected into the PVS of 48 hrs zebrafish embryos. MCF7 and MCF7 + MSCs spheroids in LG and HG ((a), left) were disaggregated, injected and visualized under fluorescence stereo microscope at time point 0 hrs post-injection ((a), right). BV = blood vessel. MCF7 dissemination in LG and HG was analyzed 72 hrs post-injection (b). White arrows indicate migrated MCF7 cells in zebrafish head and tail. Results have been presented as percentage of xenograft with invasive BC cells. Data were analyzed using the chi-square with Fisher's exact test. * denotes statistically significant values compared with MCF7 LG (* pval < 0.05). § denotes statistically significant values compared with MCF7 HG (§ pval < 0.05). ç denotes statistically significant values compared with MSC + MCF7 LG (ç pval < 0.05).

4.4 Effect of glucose-affected MSCs on MCF7 cancer stem properties

Glucose promotes the ability of adipose-derived MSC to induce BC invasiveness. CSCs play a crucial role in BC invasiveness, conferring to cancer cells the capability of anchorage-independent grown, a hallmark of metastatic potential. Thus, the effect of MSCs, and the potential role of glucose, onto MCF7 ability to grow in suspension was evaluated by measuring mammospheres formation in ultra-low attachment plates. MCF7 were plated in presence and absence of MSCs in HG or LG (4:1). After 10 days, number and diameter of mammospheres in HG or LG were determined. As shown in Figure 12, MCF7 were able to form a 2.8-fold higher number of mammospheres, also characterized by 50% increased diameter, when co-cultured with MSCs in HG, while not in LG, compared to monoculture (MCF7 LG). Thus, MSCs stimulate CSC properties in MCF7, including sphere-forming capacity in high glucose conditions.

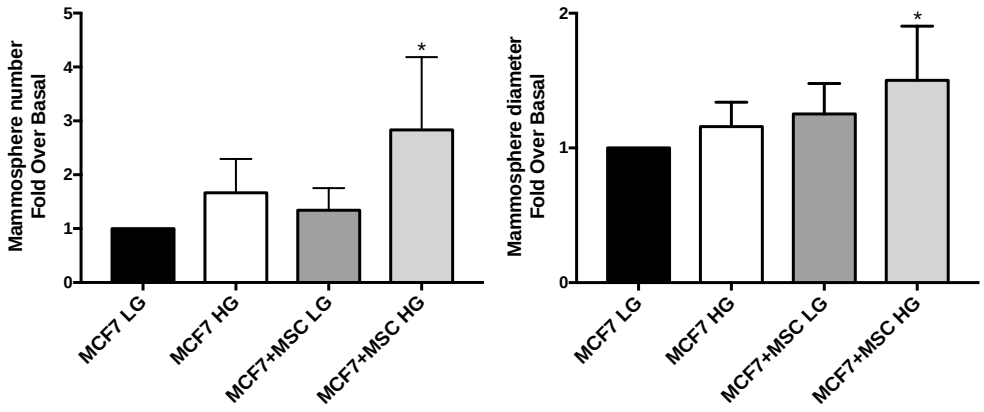

Figure 12. Effect of glucose and MSCs onto mammospheres formation. 3D-cultures were set up by using MCF7 and MSCs (ratio 4:1) in LG or HG concentrations. After 10 days, the mammosphere number and diameter were obtained. Results were reported as fold-over basal (MCF7 LG). Bars represent mean ± SD of 4-5 independent experiments showing mammosphere number and diameter, derived from BC cells, co-cultured and not with MSCs. Data were analyzed using the non-parametric Friedman test followed by Dunn's correction for multiple comparisons. * denote statistically significant values compared with MCF7 LG (*adjp<0.05)

4.5 Effect of glucose-affected MSCs in tumour recurrence

Tumour microenvironment, including MSCs, and metabolic derangements associated with, may favor the development of cancer relapse. Thus, the potential role of glucose and MSCs in breast tumour recurrence was investigated. MSCs were co-cultured with MCF7 in HG or in LG. After 72 hours, breast cancer cells were removed while MSCs were mono-cultured for further 72 hours (non-naïve MSC). Then, the ability of non-naïve MSC and MSC immediately after tumor remotion (MSCs post-co-culture) to promote MCF7 mammosphere formation was measured. Differently from naïve cells (Figure 12), MSC immediately after tumor remotion were not able to increase the MCF7 own ability to form mammospheres (no evident change in number and diameter compared to monocultured cells, independently from glucose) (Figure 13a). Of note, only in HG, MSCs non-naïve were able to promote MCF7 mammosphere formation, also characterized by increased diameter (*adjp<0.05) (Figure 13a). 3D cell viability was also evaluated in HG or LG. Interestingly, MCF7+ non-naïve MSCs-derived mammospheres showed significantly higher viability in HG than in LG (*adjp<0.05) (figure 13b).

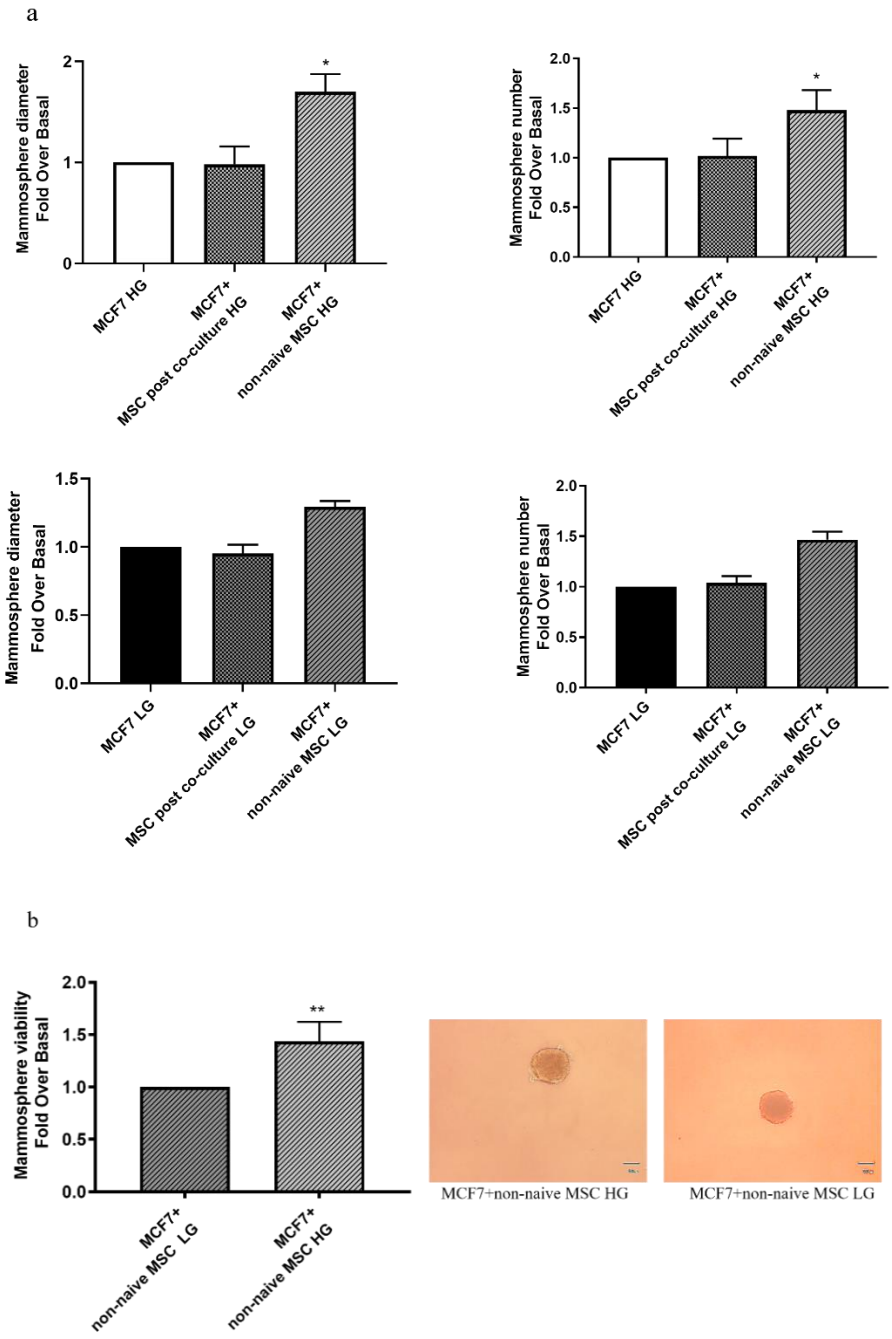

Figure 13. Glucose-modulated non-naïve MSCs effect on MCF7 ability to form mammosphere. 13a) 3D-cultures were set up by using MCF7 and MSCs post-co-culture/ non-naive MSC (ratio 4:1) in LG and HG. After 10 days, the mammosphere number and diameter were obtained. Results were reported as fold-over basal (MCF7 HG/MCF7 LG). Bars represent mean ± SD of 4-5 independent experiments showing mammosphere number and diameter in BC cells, co-cultured and not with MSC post-co-culture/non-naïve MSC. Data were analyzed using the non-parametric Kruskal-Wallis test followed by Dunn's correction for multiple comparisons. * denote statistically significant values compared with MCF7 LG (*adjp<0.05). **13b)** 3D cell viability of MCF7+ non-naïve MSC -derived spheroids was also evaluated in HG or LG. Bars represent mean ± SD of 4-5 independent experiments showing the viability of spheroids. Data were analyzed using the non-parametric Mann-Whitney test. **denote statistically significant values compared with MCF7+ non-naïve MSC LG derived-spheroids (**adjp<0.01). On the right, images of MCF7+ non-naïve MSC-derived spheroids LG/HG were obtained by microscope.

These findings suggested that, in HG, non-naïve MSC, differently from MSC immediately post-tumor remotion, promote the capability of anchorage-independent growth of MCF7.

4.6 Genetic and molecular characterization of spheroid by single-cell RNA sequencing

Metabolic changes (hyperglycemia) and the adipose-tumor microenvironment (MSCs) promote breast tumor aggressiveness and invasiveness, probably sustaining breast cancer stem cell subpopulation (BCSCs) in MCF7. As shown, glucose-affected non-naïve MSCs favour the properties of CSCs in MCF7, promoting the ability of breast cancer cells to grow under non-adherent cell culture conditions and to form spheres. To better investigate molecular and genetic identity of spheroids derived from MCF7 co-cultured with MSC non-naïve and the differences with mono-cultured MCF7, single cell RNA sequencing (sc-RNA seq) was performed. This approach allows the characterization of the cellular and molecular heterogeneity of the spheroid. Thus, MCF7 were plated in ultra-low-attachment plates to growth in anchorage-independent manner in presence and in absence of non-naïve MSC in HG. After 72 hours, obtained spheroids were analyzed by single-cell RNA sequencing. Monocultured MCF7, MSC and non-naïve MSC were analyzed as controls of spheroids. Single-cell transcriptional profiling was performed using the 10x chromium platform, followed by computational analyses with the 10X Genomics CellRanger and the Seurat software suites. Figure 14a shows an UMAP-based graphical representation of the analyzed cell types, where the different cell types are labelled according to their inputed cell identity: MCF7, MSC, non-naïve MSC and spheroid. Unsupervised global subclustering of MCF7, MSC, non-naïve MSC and spheroid, according to specific gene expression, subdivided them into six distinct clusters (figure 14b). To better understand cell samples composition of different clusters, the proportion plot is shown from ShinyCell web interface in figure 15. Each cell sample split up

into more than one cluster. Spheroid sample split up mainly into clusters 1,4, 5 and 6 and, at a lesser extent, cluster 0; MCF7 sample split up in clusters 1, 4, 5 and especially into cluster 0; MSC and non-naïve MSC samples split up in clusters 2 and 3.

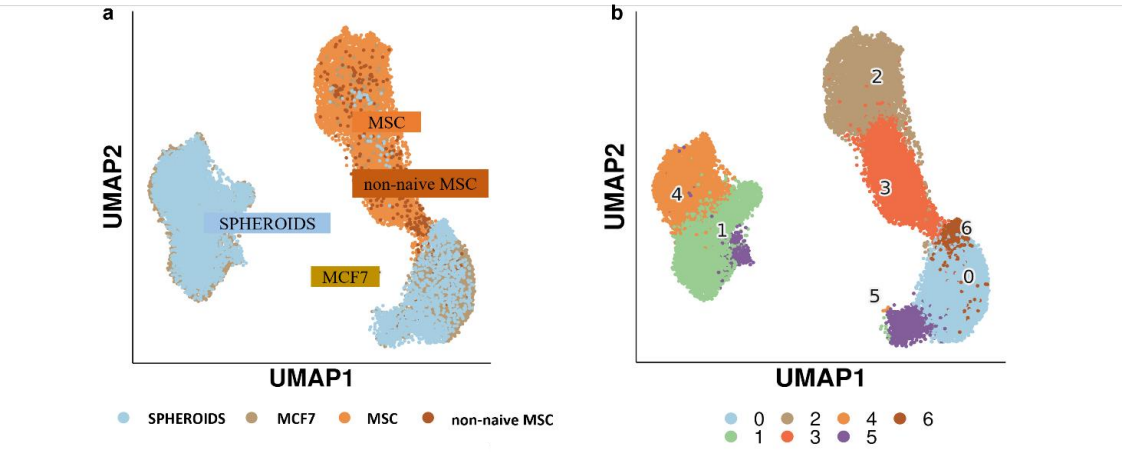

Figure 14. Clustering cell samples. 14a) UMAP plot of analyzed cell samples from sc-RNAseq colored by sample identifier. **14b)** UMAP plot of analyzed cell samples in sc-RNAseq colored by cluster. Six clusters were identified.

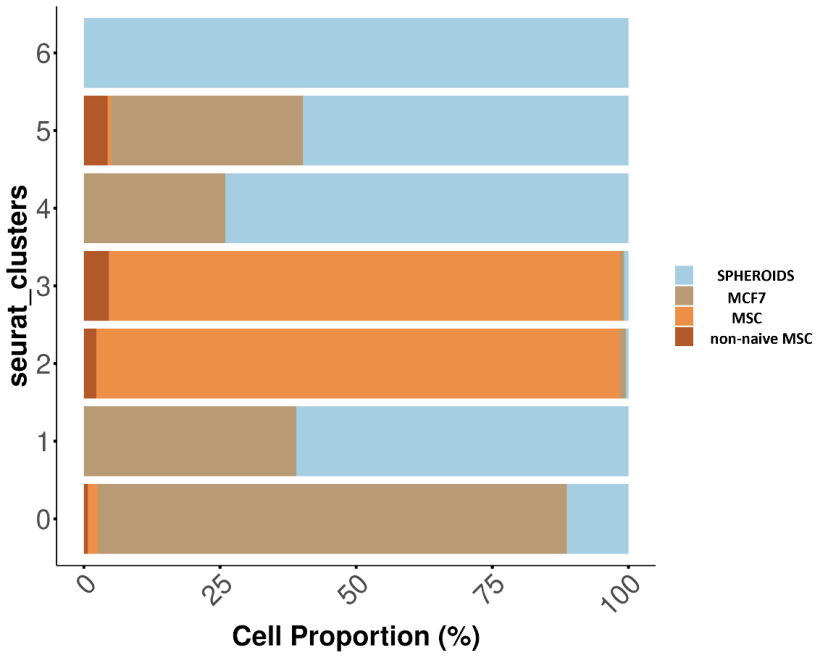

Figure 15. Proportion plot. Proportion plot indicates the percentage of cell samples (x axis) in six clusters identified (y axis). As shown, clusters 2 and 3 are composed of MSC (90% and 85%, respectively) and non-naïve MSC (5% and 10%, respectively). Clusters 0, 1 and 4 are composed of spheroids (20%, 60% and 75%, respectively) and MCF7(75%, 40% and 25%, respectively). Cluster 5 is mainly composed of spheroids (55%), but also of MCF7 (35%) and non-naïve MSC (10%). Last, cluster 6 consists only of spheroids (100%).

The top 40 of upregulated markers were identified for each cluster. To analyze the biological features of the clustered cells, gene enrichment analysis of the upregulated markers expressed in each cluster (Table1) was performed. In table 1, cell proportion %, biological process, protein class, cell types and transcription factors are reported by using different databases. The main clusters for spheroid (C1 60%, C4 75%, C5 55% and C6 100% of spheroids) revealed different biological processes such as regulation of cellular biosynthetic process and response to stimuli (C1, C4), ubiquitin-dependent protein catabolic process(C5), intracellular transport and mitochondrial ATP synthesis coupled electron transport (C6). The latter cluster (C6) shows very similar properties to cluster 0, which is mainly composed of MCF7. Indeed, C6 and C0 exhibit the same protein classes (protein scaffold, cytoskeletal protein, reductase), at least in part the same transcription factors (BRCA1, CDKN1B, MYC) and they are characterized by the same cell type (MCF7). In addition, clusters 1 and 4 mainly composed by spheroids (60% and 75%, respectively) show the same biological and molecular features, such as regulation of RNA biosynthetic process and response to stimuli and C2H2 zinc finger transcription factors, as protein class. Interestingly, cluster 5 shows the highest cellular heterogeneity (55% of spheroids, 35% of MCF7, 10% of non-naïve MSC) and unique biological processes, compared to other clusters. It is characterized by protein and macromolecule modification process and ubiquitin-dependent protein catabolic process." MCF7 breast" is the cell type identified in cluster 5, suggesting that MCF7, which constitute the spheroids, are involved in catabolic and degradation process, differently from MCF7 of cluster 1,4 and 0 involved in others process. These results highlight the presence of molecular and biological heterogeneity in breast cancer cell population. In addition, clusters 2 and 3 are mainly composed of MSC, but also non-naïve MSC (C2 90% of MSC and 5% of non-naïve MSC; C3 85% of MSC and 10% of non-naïve MSC) and corresponded to biological processes such as positive and negative regulation of biosynthetic processes, respectively. In addition, they are characterized by different expression of transcription factors (TF) target genes and interactors, such as GATA1 (C2) and TEAD4 (C3) (Table 1). These results

indicate that clusters 2 and 3 exhibit opposite biological processes, suggesting heterogeneity in cell population or that MSC might be in a cellular-state transition.

Cluster	Sample (cell proportion %)	Biological process complete (enrichmentGO Terms)	Protein class (enrichmentGO Terms)	Cell Types (ProteomicsDB 2020/CCLE Proteomics 2020/Cell Marker Augmented 2021)	Transcription Factors (Transcription Factor PPIs)
0	MCF7(75%) SPHEROIDS (20%) MSC (3%) non-naive MSC (2%)	·CELLULAR LOCALIZATION ·MITOCHONDRIAL ATP SYNTHESIS COUPLED ELECTRON TRANSPORT ·POSITIVE REGULATION OF PROTEIN TARGETING TO MITOCHONDRION	· PROTEIN SCAFFOLD, CYTOSKELETAL PROTEINS · REDUCTASE, OXIDOREDUCTASE	· MCF7 BREAST	BRCA1,CDKN1B,MYC,TP53, POU2F2
1	SPHEROIDS (60%) MCF7 (40%)	·REGULATION OF CELLULAR BIOSYNTHETIC PROCESS ·RESPONSE TO STIMULUS	· C2H2 ZINC FINGER TRANSCRIPTION FACTOR · DNA-BINDING TRANSCRIPTION FACTOR	· MCF7 BREAST · SOMATIC STEM CELL	· ZNF274,CBX3,ZBTB7B
2	MSC (90%) MSC (5%)	·POSITIVE REGULATION OF DNA-TEMPLATED TRANSCRIPTION ·POSIVITE REGULATION OF BIOSYNTHETIC PROCESS	· C2H2 ZINC FINGER FACTOR	· ENDOCRIN CELLS	· GATA1, EBF1
3	MSC (85%) non-naive MSC (10%)	·NEGATIVE REGULATION OF DNA-TEMPLATED TRANSCRIPTION ·NEGATIVE REGULATION OF BIOSYNTHETIC PROCESS	· C2H2 ZINC FINGER TRANSCRIPTION FACTOR · TRANSCRIPTIONAL COFACTORS	· HUMAN iPS · MESENCHYMAL PROGENITOR CELL: ADIPOSE TISSUE · MESENCHYMAL PROGENITOR CELL: BONE	· TEAD4,EP300
4	SPHEROIDS (75%) MCF7 (25%)	·REGULATION OF RNA BIOSYNTHETIC PROCESS ·RESPONSE TO STIMULUS	·C2H2 ZINC FINGER TRANSCRIPTION FACTOR ·DNA-BINDING TRANSCRIPTION FACTOR ·UBUIQITIN-PROTEIN LIGASE	· MCF7 BREAST · HUMAN iPS · HUMAN FIBROBLAST	· ZBTB7B
5	SPHEROIDS (55%) MCF7 (35%) non-naive MSC (10%)	·PROTEIN, MACROMOLECULE MODIFICATION PROCESS ·UBIQUITIN-DEPENDENT PROTEIN CATABOLIC PROCESS	· UBIQUITIN- PROTEIN LIGASE · CYSTEINE PROTEASE	· BREAST MCF7	· SMAD2,IRF4
6	SPHEROIDS (100%)	·CELLULAR LOCALIZATION, INTRACELLULAR TRANSPORT ·MITOCHONDRIAL ATP SYNTHESIS COUPLED ELECTRON TRANSPORT	· CYTOSKELETAL PROTEIN (TUBULIN) · PROTEIN SCAFFOLD/ADAPTOR · OXIDOREDUCTASE	· MCF7 BREAST · PROGENITOR CELL	CDKN1B,BRCA1,ESR1,ATF2, MYC, POU5F1

Table 1. Characterization of clusters. The table reports the classification and biological features of six clusters identified. Column two shows cell proportion% for each sample included per cluster. GO (gene ontology) terms significantly enriched for each cluster: biological process complete and protein class. Cell types and transcription factors of each cluster were identified by using different datasets, such as Proteomics DB 2021, CCLE Proteomics 2020, Cell Marker Augmented 2021 and Transcription Factors PPIIs dataset.

Next, to investigate further genic and molecular features of spheroids (derived from MCF7+ non-naïve MSC in HG), differentially expressed genes (DEGs) between MCF7 and spheroids was assessed. It was observed that on identified 2734 DEGs, 11% were upregulated genes with FC >0,5 and 14% were downregulated genes with FC< -0,5 in MCF7 vs spheroid (Figure 16).

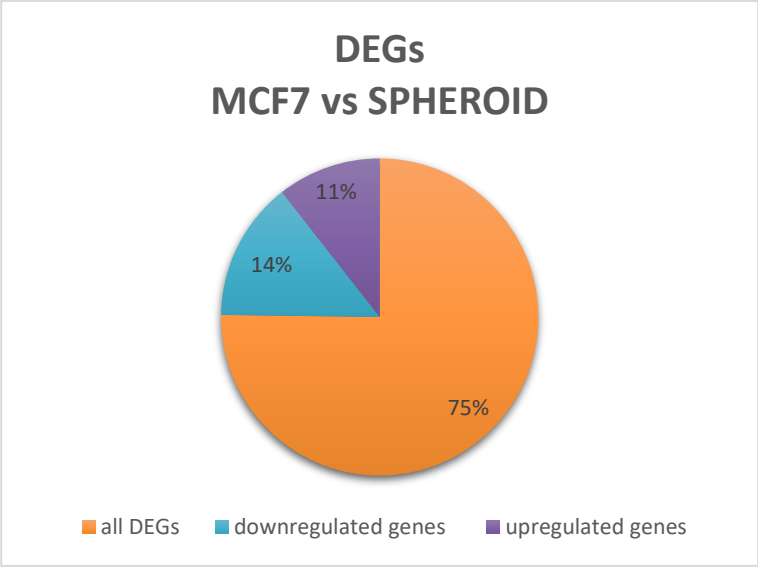

Figure 16. Pie chart. The graphic represents the percentage of up and down-regulated genes in MCF7 vs spheroid. Upregulated genes have avg_log2FC >0,5; downregulated genes have avg_log2FC<-0,5.

Next, pathway analysis was performed, using the WIKI Pathway 2021 Human and the KEGG Pathway Human 2021 databases for both up- and down-regulated genes.

At first, Wiki and KEGG pathway analysis results showed that upregulated genes are involved in different pathways, such as Cytoplasmic Ribosomal Proteins, Oxidative Phosphorylation, Mitochondrial CIV Assembly and Mitochondrial Complex I assembly (Figure 17). Furthermore, gene co-expression of two of most representative genes of each single pathway, from ShinyCell web interface, allows to visualize higher co-localization of upregulated genes in monocultured MCF7 compared to spheroids (Figure 18). *RPS26* and *RPL31* are the most representative genes for cytoplasmatic ribosomal proteins pathway; *COX6A1* and *UQCRQ* for electron transport chain pathways; *NDUFB1* and *ATP5F1E* for oxidative phosphorylation pathway; *COX6B1* and *COX8A* for mitochondrial CIV assembly. Altogether, these results suggest that monocultured MCF7 are characterized by increased biosynthetic cellular process and ATP synthesis compared to spheroids.

Figure 17. Bar chart and Manhattan Plot of upregulated genes.
Bar chart: The top 10 enriched terms for the input gene set are displayed based on the -log10(p-value). The term at the top has the most significant overlap with the input query gene set. Main pathways, where upregulated genes are involved, are cytoplasmatic ribosomal proteins, electron transport chain, oxidative phosphorylation, mitochondrial complex I and CIV assembly, proteosome etc.
Manhattan Plot: Each point represents a single term along the x-axis. The y-values represent the -log10(p-value) corresponding to the enrichment of the input gene set for the term gene set. The main pathways for upregulated genes are cytoplasmatic ribosomal proteins, electron transport chain, oxidative phosphorylation, mitochondrial complex I assembly and mitochondrial CIV assembly, proteosome etc.

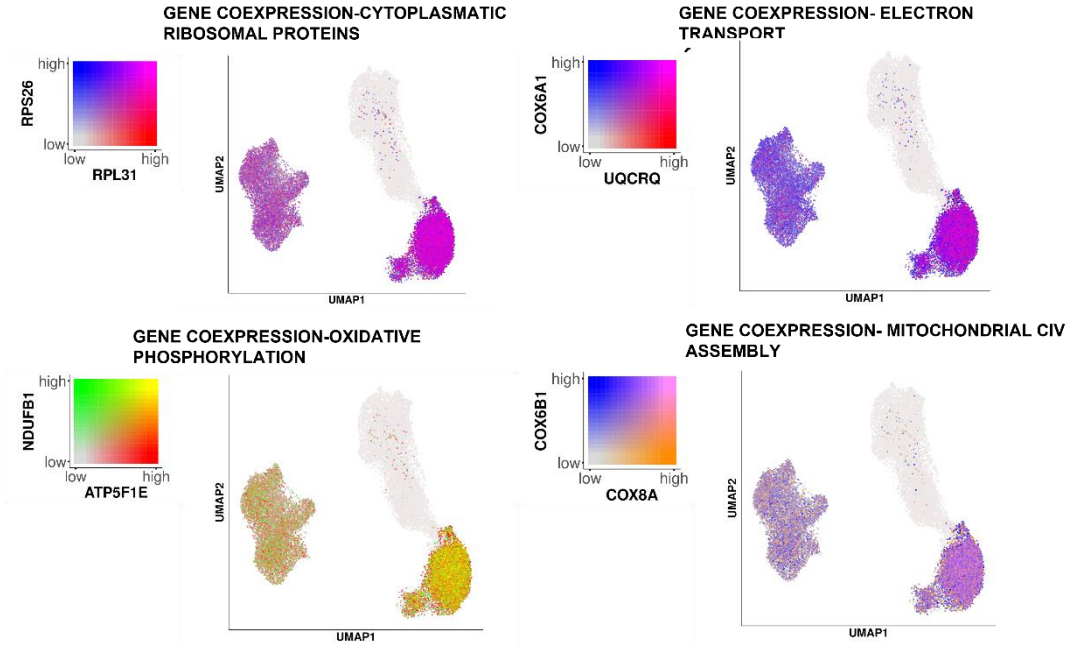

Figure 18. Upregulated genes co-expression on low-dimensional embeddings. UMAP plots generated from sc-RNA seq data showing gene co-expression levels of some representative markers of each significant pathway identified. *RPS26* and *RPL31* for cytoplasmatic ribosomal proteins pathway; *COX6A1* and *UQCRQ* for electron transport chain; *NDUFB1* and *ATP5F1E* for oxidative phosphorylation; *COX6B1* and *COX8A* for mitochondrial CIV assembly. Color of plots becomes more intense where genes are co-localization. MSC and non-naïve MSC cell samples are not shown in UMAP plots.

Conversely, downregulated genes in MCF7 vs spheroid are involved in processes promoting tumoral proliferation and metastasis formation, such as the Rap1 and ErbB signaling pathways, and pathways involved in maintaining the CSC population, such as the Wnt and Notch signaling pathways (Figure 19). In addition, the gene co-expression of two of most representative genes of each single pathway from ShinyCell web interface, allows to visualize higher co-localization of genes in spheroids compared to monocultured MCF7 (Figure 20). *CTBP2* and *MAML3* are the most representative genes for Notch pathway; *PARD6B* and *IGF1R* for Rap1 signaling pathway; *UBR5* and *SMURF2* for ubiquitin mediated proteolysis; *PLCB1* and *TBL1X* for Wnt signaling pathway; *ASH1L* and *EHMT1* for Histone modifications; *ERBB4* and *ABL1* for ErbB pathway.

Wiki Pathway 2021 Human
Table

Index	Name	P-value	Adjusted p-value	Odds Ratio	Combined score
1	Pathways affected in adenoid cystic carcinoma WP3651	6.368e-12	2.050e-9	12.67	326.53
2	Endoderm differentiation WP2853	7.773e-7	0.0001251	4.95	69.57
3	Mesodermal commitment pathway WP2857	0.00002869	0.003080	4.05	42.35
4	Rett syndrome causing genes WP4312	0.0002177	0.01752	6.51	54.88
5	Pilocytic astrocytoma WP2253	0.0003240	0.02087	37.90	304.50
6	ErbB signaling pathway WP673	0.0005755	0.03089	4.19	31.27
7	Ectoderm Differentiation WP2858	0.0009305	0.04280	3.31	23.13
8	DNA IR-damage and cellular response via ATR WP4016	0.001072	0.04314	4.24	28.98
9	Biotin Metabolism (including IEMs) WP5031	0.001284	0.04595	18.95	126.14
10	PKC gamma calcium signaling pathway in ataxia WP4760	0.002229	0.04611	8.43	51.48
11	Signaling of Hepatocyte Growth Factor Receptor WP313	0.001695	0.04611	6.55	41.80
12	Histone Modifications WP2369	0.001687	0.04611	4.44	28.37
13	Androgen receptor signaling pathway WP138	0.002291	0.04611	3.72	22.60
14	Thermogenesis WP4321	0.001955	0.04611	3.47	21.64
15	Breast cancer pathway WP4262	0.002250	0.04611	2.94	17.93
16	Focal Adhesion WP306	0.001994	0.04611	2.69	16.73
17	Nanoparticle triggered autophagic cell death WP2509	0.002644	0.05009	7.99	47.41
18	DNA IR-double strand breaks and cellular response via ATM WP3959	0.002874	0.05142	4.66	27.25
19	Thyroid hormones production and their peripheral downstream signaling effects WP4746	0.003214	0.05446	3.50	20.11
20	Leptin signaling pathway WP2034	0.003479	0.05601	3.86	21.86
21	Chemokine signaling pathway WP3929	0.003658	0.05609	2.75	15.41
22	Fragile X Syndrome WP4549	0.004212	0.06164	3.06	16.76
23	Notch Signaling Pathway Netpath WP61	0.004836	0.06771	4.15	22.11
24	Autophagy WP4923	0.007098	0.07150	5.84	28.87
25	Notch Signaling WP268	0.005901	0.07150	4.75	24.36

KEGG Pathway Human 2021
Table

Index	Name	P-value	Adjusted p-value	Odds Ratio	Combined score
1	Ubiquitin mediated proteolysis	0.000003541	0.0007789	4.63	58.08
2	Lysine degradation	0.00003289	0.003618	6.37	65.80
3	Rap1 signaling pathway	0.0001200	0.008800	3.18	28.67
4	Estrogen signaling pathway	0.0002335	0.01270	3.68	30.77
5	Thyroid hormone signaling pathway	0.0003055	0.01270	3.83	30.99
6	ErbB signaling pathway	0.0003465	0.01270	4.52	36.05
7	Homologous recombination	0.0006042	0.01899	6.52	48.36
8	Focal adhesion	0.0007711	0.02120	2.87	20.59
9	Sphingolipid signaling pathway	0.001049	0.02565	3.51	24.05
10	Fanconi anemia pathway	0.002617	0.05404	4.75	28.27
11	Proteoglycans in cancer	0.002702	0.05404	2.59	15.33
12	Growth hormone synthesis, secretion and action	0.003772	0.05896	3.12	17.41
13	Wnt signaling pathway	0.004010	0.05896	2.71	14.96
14	Notch signaling pathway	0.004097	0.05896	4.30	23.66
15	Chemokine signaling pathway	0.004351	0.05896	2.55	13.86
16	Hepatocellular carcinoma	0.004388	0.05896	2.68	14.53
17	Regulation of actin cytoskeleton	0.004556	0.05896	2.43	13.08
18	Breast cancer	0.004954	0.06055	2.79	14.78
19	Parathyroid hormone synthesis, secretion and action	0.006243	0.07229	3.11	15.78
20	Cortisol synthesis and secretion	0.006600	0.07260	3.87	19.41
21	Vascular smooth muscle contraction	0.007750	0.08119	2.77	13.44
22	Cholinergic synapse	0.009070	0.08923	2.90	13.64
23	Autophagy	0.009328	0.08923	2.68	12.52
24	Endocrine and other factor-regulated calcium reabsorption	0.01172	0.1014	3.95	17.58
25	Human papillomavirus infection	0.01274	0.1014	1.94	8.48

Manhattan Plot

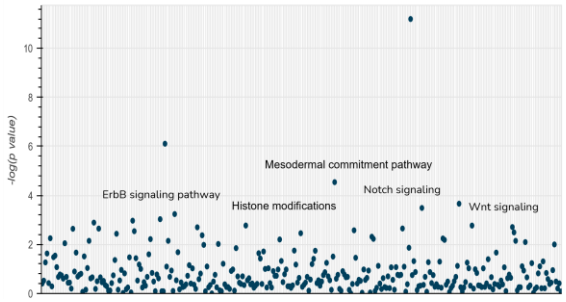

Manhattan Plot

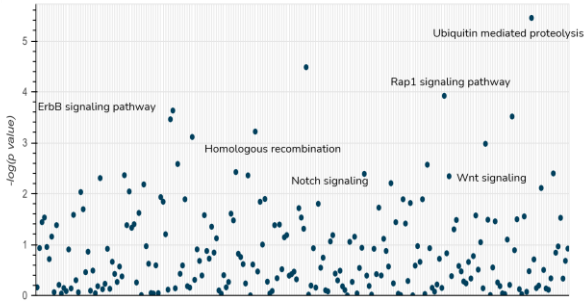

Figure 19. Table and Manhattan Plot of downregulated genes.
Table: top 25 of pathways identified ranked in order of significant pvalue. The most significant pathways are Ubiquitin mediated proteolysis, Histone modifications, Rap1 signaling pathway, ErbB signaling pathway, Homologus recombination, Notch signaling pathway, Wnt signaling pathway etc. **Manhattan Plot:** Each point represents a single term along the x-axis. The y-values represent the -log10(p-value) corresponding to the enrichment of the input gene set for the term gene set. Main pathways where upregulated genes are involved are Ubiquitin mediated proteolysis, Histone modifications, Rap1 signaling pathway, ErbB signaling pathway, Homologus recombination, Notch signaling pathway, Wnt signaling pathway etc.

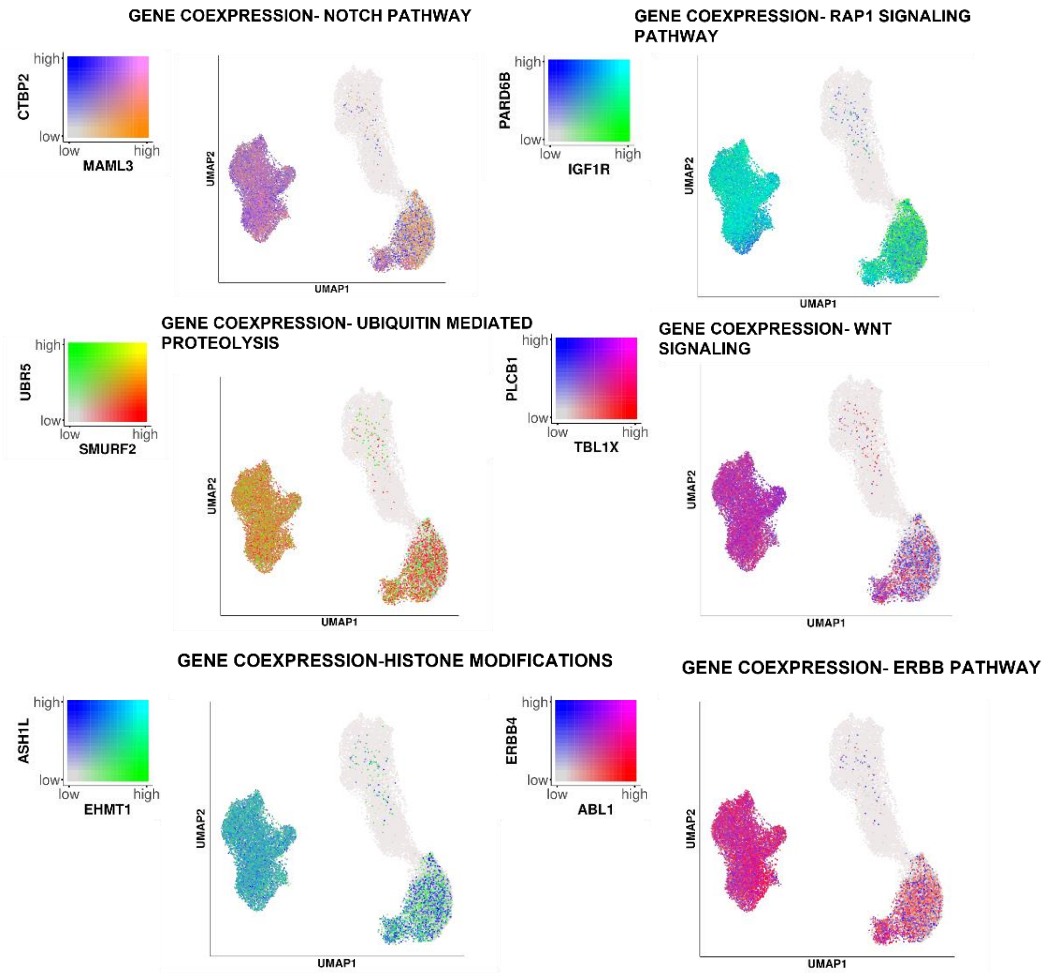

Figure 20. Down-regulated genes co-expression on low-dimensional embeddings. UMAP plots generated from sc-RNA seq data showing gene co-expression levels of some representative markers of each significant pathway identified. *CTBP2* and *MAML3* for Notch pathway; *PARD6B* and *IGF1R* for Rap1 signaling pathway; *UBR5* and *SMURF2* for Ubiquitin mediated proteolysis; *PLCB1* and *TBL1X* for Wnt signaling pathway; *ASH1L* and *EHMT1* for Histone modifications; *ERBB4* and *ABL1* for ERBB pathway. Color of plots become more intense where genes are co-localization. MSC and non-naïve MSC cell samples are not shown in UMAP plots.

Thus, upregulation of pro-metastatic and pro-tumorigenic pathways (Rap 1 and ErbB, Notch and Wnt pathways) in spheroid compared to monocultured MCF7 may confirm the presence of BCSCs population in MCF7 co-cultured with non-naïve MSC (spheroids), according with previously demonstrated results. Thus, glucose-affected mesenchymal stem cells promote the acquisition of stem phenotype in MCF7.

5. Discussion and conclusions

Type 2 diabetes (T2D) is one of the most prevalent chronic metabolic disorders characterized by hyperglycemia (100). Dysfunction of pancreatic insulin-producing β-cells and insulin resistance mainly leads to hyperglycemia, resulting in an increased risk of T2D development. T2D may be associated with increased risk, accelerated progression and mortality rates of several types of cancer, including breast cancer (101). In breast cancer, hyperglycemia correlates with an increased prevalence and mortality but also has a major impact on chemotherapy's efficacy, leading to chemoresistance (102). Studies have reported that high glucose concentrations significantly increase the proliferation of BC cells (103). A high blood glucose level in tumor microenvironment is crucial in tumour growth. Breast cancer cells are mainly surrounded by mammary adipose tissue with various stromal cells such as MSCs, fibroblasts, endothelial, and immune cells. Hyperglycemia causes several changes in the microenvironment, such as the increase in pH, the high concentration of lactic acid, the imbalance of ROS and the impact on immune cells. Diabetes-associated hyperglycemia alters adipose tissue's metabolic profile and leads to the increased secretion of numerous hormones, adipokines, inflammatory cytokines, growth factors, enzymes and free fatty acids (104). Adipose tissue-specific altered secretions contribute to the initiation and progression of breast cancer. Adipose tissue contains Mesenchymal stem cells, a plastic-adherent fibroblastic cell population, that exhibit a defined immunophenotype (e.g. expression of mesenchymal stem markers CD73, CD90, CD105 and lack of expression of hematopoietic/endothelial markers), and ability of clonal differentiation towards mesenchymal lineages (e.g., adipogenic, osteogenic and chondrogenic lineages) (105). In breast, MSCs play a crucial role in promoting tumor progression. MSC-secreted factors, that accompany tissue regeneration and revascularization have also been linked to the promotion of cancer growth and metastasis. Established communication between cancer cells and adipocytes and their mesenchymal precursors provides mechanical and energy support for breast cancer cells. Hyperglycemia may affect this communication, contributing to the association between metabolic diseases and BC progression.

Previously, it was demonstrated that glucose promotes adipocyte release of IGF1, CCL5 and IL-8, enhancing BC cell proliferation, invasiveness and tamoxifen resistance (106,57-59). Recent works have focused on identifying and elucidating the mechanisms that drive the emergence of cancer-initiating cells, known as cancer stem cells (CSCs), which appear to contribute to forming distant metastasis and chemoresistance. Emerging data suggest that the tumor microenvironment can influence their prevalence (107). Several studies evidenced that breast cancer stem cells exist in cells with a surface stem profile of $CD44^{high}/CD24^{low}$ phenotype (108). Thus, the ability of adipose-microenvironment-derived MSCs to promote the acquisition of stem features in MCF7 and the potential role of glucose in this interaction was evaluated. At first 2D system was established, where MCF7 were co-cultured with MSCs and exposed to high glucose or low glucose concentrations. It was observed that glucose influences the ability of MSCs to induce stem-like phenotype in MCF7 cells, increasing the percentage of $CD44^{high}/CD24^{low}$ BC subpopulation in high glucose conditions. Normal stem cells and CSCs share some normal stem cells features. They possess the capacity of self-renewal to give rise to highly proliferative cells and more differentiated cancer cells representing several lineages and constituting the bulk of heterogeneous tumour. The cancer stem cell (CSCs) theory implies that CSCs can express pluripotency genes such as *OCT4*, *SOX2* and *NANOG*. Aberrant gene expression causes continuous self-renewal circuit activation, leading to oncogenic transformation, tumour initiation and maintenance (109). Thus, to further investigate MSCs-induced stem phenotype of MCF7, it was analyzed the expression levels of master regulators of stemness, *OCT4*, *SOX2* and *NANOG*. Data showed an increased gene expression of *OCT4* in MCF7 co-cultured with MSCs only in HG, suggesting for the first time that glucose promotes the acquisition of stem features in MCF7 in presence of MSCs. Compared with other stemness genes, *OCT4* has universal expression in CSCs of breast cancer. It seems that *OCT4* can be used to distinguish from non-CSCs, and participate in determining the biological function of CSCs (110). To define bi-directional communication between cancer cells and adipose-derived MSCs, the impact of glucose and of MCF7 onto MSCs multipotency was investigated in the same

system. It was observed that co-cultures with MCF7 significantly reduced mRNA levels of *OCT4* and *SOX2* only in HG, suggesting an MCF7-induced loss of multipotency in MSCs. To better understand the dialogue between MCF7 and adipose-derived MSCs, 3D system was established. The utility of the 3D culture models to explore aspects of the malignant phenotype in culture has now been widely recognized. Many works have adopted these approaches to study breast cancers (111). 3D in vitro models that mimic the tumour microenvironment are crucial for developing treatment strategies and studying the molecular mechanisms behind tumor formation, progression and metastasis (112). Thus, MCF7 were grown in anchorage-independent manner by plating them in ultra-low-attachment plates in presence and absence of MSCs. Obtained spheroids were mechanically disaggregated to measure OCT4 protein expression in both MCF7 and MSCs. Spheroids-derived MCF7 and MSCs displayed increased and reduced OCT4 protein expression, respectively, in HG while not in LG. Such data confirmed that glucose interferes with MCF7-MSCs communication, inducing the acquisition of a stem phenotype in MCF7 and the loss of multipotency in MSCs. Moreover, patients with high OCT4 expression in BC showed poor post-progression survival (113). The aberrant expression of this pluripotency TFs governs tumorigenesis and aids malignancy, therefore representing a promising therapeutic target to eradicate CSCs specifically. The reduction of multipotency markers represents the loss of an undifferentiated state of MSCs, leading to the investigation of phenotypic changes, such as potential acquisition of myofibroblastic and senescent features in MSCs upon co-culture with MCF7. A significantly increased expression of fibroblast markers FAP and a-SMA was observed either in 2D and in 3D systems only in HG. Such data indicate that glucose promotes the acquisition of fibrotic phenotype in MSCs co-cultured with MCF7. Cancer-associated fibroblasts (CAFs) play an important role in the growth of solid epithelial tumours. Expression of various “CAF markers”, such as FAP and α-SMA separates them from the larger pool of fibroblasts present in breast cancer stroma. MCF7-induced CAF features in MSC were also accompanied by an altered expression of senescent markers, *LMNB1* and *CDKN2A* (the latter also at protein levels-p16 protein-) only in HG. In addition, it was demonstrated that

senescence in tumor microenvironment is a primary cause of therapy resistance and cancer relapse (90). Thus, observed phenotypic changes in MSCs suggest that glucose promotes the transdifferentiation of MSCs in senescent CAFs. In recent years, senescent CAFs have become a novel target in cancer treatment (114). Senescent fibroblasts within the tumor microenvironment and cancer-associated fibroblasts (CAFs) promote every step of the transformation process by stimulating tumor growth, angiogenesis, invasion, and metastasis (115). Thus, a glucose-modulated pro-metastatic effect of MSCs on MCF7 was investigated by establishing a zebrafish xenograft model. Zebrafish represents a metastatic animal model used to evaluate the ability of cancer cell migration. Therefore, spheroid-derived MCF7 and MSC cells were injected in zebrafish embryos, which are optically transparent and permissive to the xenograft of human tumor cells. This method allows in vivo delivery of a very limited number of cancer cells, mimicking the initial stages of tumor angiogenesis and metastasis; thus, it is now considered a useful approach to study the metastatic homing and colonization (68–69). Here, it was observed that the injection of spheroid-derived MCF7+MSCs led to higher tumor invasiveness compared to spheroid-derived monocultured MCF7, only in HG. Indeed, in LG the percentage of xenografts with invasive cells was significantly lower. This model allows to study the communication between MSC and tumoral cells during cancer cell invasion and metastasis and may be envisioned as a novel approach for drug screening toward breast cancer. Thus, glucose promotes the ability of adipose-derived MSC to promote breast cancer invasiveness, probably sustaining CSCs population in MCF7 cells. Another important CSCs feature, such as the ability to grow in anchorage-independent manner, was demonstrated. MSC+MCF7-derived spheres were characterized by increased number and diameter compared to MCF7 alone-derived spheres, only in HG, while not in LG. Such data confirm that glucose-affected MSCs promote CSCs population in MCF7. Increasing evidence has proven the crucial role of breast CSCs, not only in tumor initiation, progression, metastasis and drug resistance, but also in tumor recurrence (116). To investigate the behaviour of adipose microenvironment in tumor relapse, tumor recurrence was simulated by using both 2D and 3D systems. MSCs were co-cultured with MCF7 in HG or in

LG. After 72 hours, breast cancer cells were removed, while MSCs were mono-cultured for further 72 hours (non-naïve MSC). MSC, immediately after tumor remotion, were unable to increase the MCF7 own ability to form spheres. At variance, non-naïve MSCs were able to promote MCF7 sphere formation, also characterized by increased diameter, only in HG. Thus, non-naive MSCs, probably, show different features compared to MSC immediately post-co-cultures. To better understand molecular and genic features of MCF7+non-naïve MSC derived spheroids in high glucose condition, spheroids were characterized by using single-cell RNA sequencing. Assessing the gene expression difference between individual cells could identify rare populations, that cannot be detected from an analysis of pooled cells. For example, finding and characterizing outlier cells within a population has potential implications for understanding drug resistance and relapse in breast cancer treatment (117). In addition, molecular and genetic heterogeneity is increasingly recognized in many tumors and can contribute considerably to drug resistance. The emergence of single-cell RNA sequencing (scRNA-seq) technology can detect and decode the heterogeneity of breast cancer cells, refine molecular types, and open up new ways to overcome resistance (118). Unsupervised clustering allowed to subdivide cell samples (MSC, non-naïve MSC, MCF7 and spheroid, which corresponds to mixed populations of MCF7+non-naïve MSCs), according to specific gene expression, in different six clusters. These clusters are characterized by molecular and biological differences, suggesting heterogeneous populations or different transition states in cell populations analyzed. Interestingly, clusters 1,4,5,6 and 0 are composed by spheroids and MCF7 samples. Clusters 1 and 4 are characterized by the regulation of biosynthetic process and response to stimuli, by zinc finger transcription factors (as protein class) and MCF7 breast (as cell types). Cluster 5 showed unique features; indeed, it is characterized by catabolic and protein modification process, by ubiquitin-protein ligase and cysteine protease and by MCF7 breast (as cell types). Cluster 6 is different from clusters 1,4 and 5, but similar to cluster 0; both are characterized by intracellular transport and mitochondrial ATP synthesis, by same proteins scaffold and oxidoreductase and mainly by MCF7 (as cell types). Thus, these analyzed clusters are mainly

represented by MCF7 samples and show different features, suggesting a molecular and biological heterogeneity in MCF7 cell population either in monoculture either in spheroids cell samples. MSC sample split up in cluster 2 and 3, but these clusters are different from each other; for example their upregulated markers are involved in opposite biological processes, like positive and negative regulation of biosynthetic processes (clusters 2 and 3, respectively) and are represented by different Cell types (endocrine cells and mesenchymal progenitor cells, respectively). These results suggest that MSC might be in a cellular-state transition in cluster 2, where they are less stem and able to release secreted factors compared to those in cluster 3. Such analysis indicates heterogeneity in MSC cell population. sc-RNA seq allowed to assess of differentially expressed genes (DEG) between monocultured MCF7 and spheroids, identifying down and up-regulated genes. Pathways analysis of upregulated genes in monocultured MCF7 compared to spheroids identified pathways, such as Cytoplasmic Ribosomal Proteins, Oxidative Phosphorylation, Electron Transport Chain, Mitochondrial CIV Assembly and Mitochondrial Complex I assembly. Thus, monocultured MCF7 are characterized by increased biosynthetic cellular process and ATP synthesis, suggesting that breast cancer cells, in response to high glucose concentration, alter metabolic processes to sustain their uncontrolled growth and proliferation and their survival. Interestingly, pathway analysis of genes in monocultured MCF7 vs spheroids allowed to identify upregulated pro-tumorigenic and pro-metastatic pathways (such as ErbB and Rap1 signaling pathways) in spheroids. Aberrant signalling of ErbB family members in cancer cells contributes to tumour development via the following two aspects: augmented cell growth and survival (119). Ras-associated protein-1(Rap1) plays important roles in regulating multiple key events in tumor cell migration, invasion, and metastasis. Rap1 activation promotes the adhesion of lymphoma cells to transmigration into the hematopoietic system, through which lymphoma cells spread to distant organs. (120). In addition, Wnt and Notch signaling pathways were also upregulated in spheroids compared to monocultered MCF7. Both pathways play a crucial role in self-renewal and maintenance of CSC subpopulation in breast cancer cells. Thus, MCF7 co-cultured with MSCs in HG (spheroids) seem to be more aggressive than monocultured

MCF7. Thus, the single-cell analysis may evidence a likely horizontal transfer of stemness potential from MSCs to MCF7 cells, resulting in the acquisition of stronger pro-tumorigenic and pro-metastatic phenotypes. Several pathways are operative in breast CSCs to maintain their stemness such as Notch, Hedgehog, Wnt, etc. Dysfunction of these stemness signaling pathways moderates self-renewal characteristics, thus leading to the detainment of CSC phenotype. Aberrant activation or mutation in stemness-related genes is frequently reported and associated with aggressiveness and cancer relapse. Notch, Hedgehog, Wnt signaling pathways can interact through cross-talk as part of complex signaling networks. Cross-talk may also contribute to the cellular diversity and may have a key role in the growth of CSCs. The identification of crosstalk networks can provide new opportunities for designing more effective treatment regimens (121). In addition, accumulated evidence suggests that stromal cells such as fibroblasts, macrophages, mesenchymal stem cells (MSCs) and tumour-associated endothelial cells play an imperative role in driving these pathways for enrichment and maintenance of breast CSCs signaling (122).

In conclusion, it was demonstrated how glucose-modulated MSCs promote stem properties in ER^+ breast cancer cells, MCF7, increasing the prevalence of CSCs population and favouring their maintenance. In parallel, glucose-affected breast cancer cells induce phenotypic changes in MSCs, promoting the loss of multipotency and acquisition of fibrotic and senescent features. Such results indicate that glucose interferes with communication between MSCs and MCF7. Thus, tumor-educated MSCs sustain CSCs population in MCF7, promoting self-renewal characteristics, metastatic potential, and the ability to anchorage-independent growth, only in HG. In addition, CSCs display immense potential to migrate to various body parts through blood circulation, becoming responsible for drug resistance and cancer relapse, where the recurrent form is more aggressive and not easily curable. Therefore, identifying CSC-specific signaling networks is essential for improving anti-CSC cancer therapy (123). In keeping with the findings of this PhD work, investigating Notch and Wnt signaling pathways, identified by sc-RNA seq in MCF7 co-cultured in high glucose condition, will

allow determining specific molecular targets for the treatment of diabetic subjects affected by breast cancer.

6. References

1. National Center for Health Statistics. Mortality multiple cause micro-data files, 2015: public-use data file and documentation: NHLBI tabulations. https://www.cdc.gov/nchs/nvss/mortality_public_use_data.htm. Accessed 23 Dec 2018.
2. Centers for Disease Control and Prevention. National diabetes fact sheet: national estimates and general information on diabetes and prediabetes in the United States, 2011. Atlanta: US Department of health and human services, Centers for Disease Control and Prevention; 2011.
3. Dokken B. The pathophysiology of cardiovascular disease and diabetes: beyond blood pressure and lipids. Diabetes Spectr. 2008;21(3):160–5.
4. Guasch-Ferré, M.; Hruby, A.; Toledo, E.; Clish, C.B.; Martínez-González, M.A.; Salas-Salvadó, J.; Hu, F.B. Metabolomics in Prediabetes and Diabetes: A Systematic Review and Meta-analysis. Diabetes Care 2016, 39,833–846.
5. Hu, F.B.; Satija, A.; Manson, J.E. Curbing the diabetes pandemic: The need for global policy solutions. JAMA 2015, 313, 2319–2320.
6. Biomarkers for type 2 diabetes. MarkkuLaakso. Review. Molecular Metabolism. Volume 27, Supplement, September 2019, Pages S139-S146.
7. Chatterjee, S., Khunti, K., Davies, M.J., 2017. Type 2 diabetes. Lancet 389: 2239e2251.
8. Hu, F.B.; Satija, A.; Manson, J.E. Curbing the diabetes pandemic: The need for global policy solutions. JAMA 2015, 313, 2319–2320.
9. E. Giovannucci, D.M. Harlan, M.C. Archer, R.M. Bergenstal, S.M. Gapstur, L.A. Habel, M. Pollak, J.G. Regensteiner, D. Yee, Diabetes and cancer: a consensus report, Diabetes care 33 (7) (2010) 1674–1685.
10. C.-X. Xu, H.-H. Zhu, Y.-M. Zhu, Diabetes and cancer: Associations, mechanisms, and implications for medical practice, World J. Diabetes 5 (3) (2014) 372–380
11. A. Mantovani, G. Targher, Type 2 diabetes mellitus and risk of hepatocellular carcinoma: spotlight on nonalcoholic fatty liver disease, Ann. Transl. Med. 5 (13) (2017) 270
12. Kang C, LeRoith D, Gallagher EJ. Diabetes, Obesity, and Breast Cancer. *Endocrinology* (2018) 159(11):3801–12. 10.1210/en.2018-00574.
13. Hardefeldt PJ, Edirimanne S, Eslick GD. Diabetes increases the risk of breast cancer: a meta-analysis. Endocr Relat Cancer 2012;19(6):793–803.
14. Boyle P, Boniol M, Koechlin A, Robertson C, Valentini F, Coppens K, et al. Diabetes and breast cancer risk: a meta-analysis. Br J Cancer 2012;107(9):1608–17.
15. Hu K., Ding P., Wu Y., Tian W., Pan T., Zhang S. Global patterns and trends in the breast cancer incidence and mortality according to sociodemographic indices: An observational study based on the global burden of diseases. *BMJ Open.* 2019;9:e028461. doi: 10.1136/bmjopen-2018-028461.
16. Fan Zhang, Jing de Haan-Du, Grigory Sidorenkov, Gijs W. D. Landman, Mathilde Jalving, Qingying Zhang and Geertruida H. de Bock1. Type 2 Diabetes Mellitus and Clinicopathological Tumor Characteristics in Women

Diagnosed with Breast Cancer: A Systematic Review and Meta-Analysis. Cancers(Basel). 2021 Oct; 13(19): 4992. doi: 10.3390/cancers13194992

17. Fitzmaurice, C.; Abate, D.; Abbasi, N.; Abbastabar, H.; Abd-Allah, F.; Abdel-Rahman, O.; Abdelalim, A.; Abdoli, A.; Abdollahpour, I.; et al.; Global Burden of Disease Cancer Collaboration. Global, Regional, and National Cancer Incidence, Mortality, Years of Life Lost, Years Lived With Disability, and Disability-Adjusted Life-Years for 29 Cancer Groups, 1990 to 2017: A Systematic Analysis for the Global Burden of Disease Study. JAMA Oncol. 2019, 5, 1749–1768.
18. Ferlay, J.; Laversanne, M.; Ervik, M.; Lam, F.; Colombet, M.; Mery, L.; Piñeros, M.; Znaor, A.; Soerjomataram, I.; Bray, F. Global Cancer Observatory: Cancer Tomorrow. 12 June 2021.
19. Starup-Linde, J.; Karlstad, O.; Eriksen, S.A.; Vestergaard, P.; Bronsveld, H.K.; de Vries, F.; Andersen, M.; Auvinen, A.; Haukka, J.; Hjellvik, V.; et al. CARING (CAncer Risk and INsulin analoGues): The association of diabetes mellitus and cancer risk with focus on possible determinants—a systematic review and a meta-analysis. Curr. Drug Saf. 2013, 8, 296–332.
20. Zhou, Y.; Zhang, X.; Gu, C.; Xia, J. Influence of diabetes mellitus on mortality in breast cancer patients. ANZ J. Surg. 2015, 85, 972–978.
21. Jasmine Gajeton, Irene Krukovets, Santoshi Muppala, Dmitriy Verbovetskiy, Jessica Zhang and Olga Stenina-Adognravi. Hyperglycemia-Induced miR-467 Drives Tumor Inflammation and Growth in Breast Cancer. Cancers (Basel). 2021 Mar; 13(6): 1346. doi: 10.3390/cancers13061346
22. Coussens L.M., Werb Z. Inflammation and cancer. *Nature.* 2002;420:860–867. doi: 10.1038/nature01322.
23. Zhao X.B., Ren G.S. Diabetes mellitus and prognosis in women with breast cancer: A systematic review and meta-analysis. *Medicine.* 2016;95:e5602. doi: 10.1097/MD.0000000000005602
24. Mohamed HT, El-Shinawi M, Nouh MA, Bashtar AR, Elsayed ET, Schneider RJ, et al. Inflammatory breast cancer: high incidence of detection of mixed human cytomegalovirus genotypes associated with disease pathogenesis. *Front Oncol* (2014) 4:246. 10.3389/fonc.2014.00246
25. Samuel SM, Varghese E, Varghese S, Büsselberg D. Challenges and perspectives in the treatment of diabetes associated breast cancer. *Cancer Treat Rev* (2018) 70:98–111. 10.1016/j.ctrv.2018.08.004
26. Warburg O. On the origin of cancer cells. *Science* (1956) 123:309–14. 10.1126/science.123.3191.309
27. Yang L, He Z, Yao J, Tan R, Zhu Y, Li Z, et al.. Regulation of AMPK-related glycolipid metabolism imbalances redox homeostasis and inhibits anchorage independent growth in human breast cancer cells. *Redox Biol* (2018) 17:180–91. 10.1016/j.redox.2018.04.016
28. Ferroni P, Riondino S, Buonomo O, Palmirotta R, Guadagni F, Roselli M. Type 2 diabetes and breast cancer: the interplay between impaired glucose metabolism and oxidant stress. Oxid Med Cell Longev 2015;2015:183928.
29. Burstein HJ, Krilov L, Aragon-ching JB, et al. Clinical cancer advances 2017 : annual report on progress against cancer from the American Society of Clinical Oncology. *J Clin Oncol*. 2017;35:1342–1368.

30. Werner HMJ, Mills GB, Ram PT. Cancer systems biology: A peek into the future of patient care? *Nat Rev Clin Oncol*. 2014;11:1–22.
31. Lindeman, G.J., Visvader, J.E., 2010. Insights into the cell of origin in breast cancer and breast cancer stem cells. Asia-Pac. J. Clin. Oncol. 6, 89-97.
32. Kreso, A., Dick, J.E., 2014. Evolution of the cancer stem cell model. Cell Stem Cell. 14, 275-291. https://doi.org/ 10.1016/j.stem.2014.02.006.
33. De Beça, F.F., Caetano, P., Gerhard, R., Alvarenga, C.A., Gomes, M., Paredes, J., Schmitt, F., 2013. Cancer stem cells markers CD44, CD24 and ALDH1 in breast cancer special histological types. J. Clin. Pathol. 66, 187-191. https://doi.org/ 10.1136/jclinpath-2012-201169
34. Senbanjo, L.T., Chellaiah, M.A., 2017. CD44: a multifunctional cell surface adhesion receptor is a regulator of progression and metastasis of cancer cells. Front. Cell. Dev. Biol. 5, 18. https://doi.org/10.3389/fcell.2017.00018.
35. Kwon, M.J., Han, J., Seo, J.H., Song, K., Jeong, H.M., Choi, J.S., Kim, Y.J., Lee, S.H., Choi, Y.L. and Shin, Y.K., 2015. CD24 overexpression is associated with poor prognosis in luminal A and triple-negative breast cancer. PLoS One. 10, e0139112.
36. Li, W., Ma, H., Zhang, J.,Zhu, L., Wang, C., Yang, Y., 2017. Unraveling the roles of CD44/CD24 and ALDH1 as cancer stem cell markers in tumorigenesis and metastasis. Sci. Rep.7, 13856. https://doi.org/10.1038/s41598-017-14364-2.
37. Sheridan C, et al. CD44+/CD24− breast cancer cells exhibit enhanced invasive properties: an early step necessary for metastasis. *Breast Cancer Res.* 2006;**8**:R59. doi: 10.1186/bcr1610.
38. Moreb, J.S., Ucar, D., Han, S., Amory, J.K., Goldstein, A.S., Ostmark, B., Chang, L.J., 2012. The enzymatic activity of human aldehyde dehydrogenases 1A2 and 2 (ALDH1A2 and ALDH2) is detected by Aldefluor, inhibited by diethylaminobenzaldehyde and has significant effects on cell proliferation and drug resistance. Chem. Biol. Interact. 195, 52-60.
39. Reya T, Morrison SJ, Clarke MF, Weissman IL. Stem cells, cancer, and cancer stem cells. Nature 2001;414:105–11.
40. Ramesh Butti 1, Vinoth Prasanna Gunasekaran 2, Totakura V S Kumar 3, Pinaki Banerjee 4, Gopal C Kundu. Breast cancer stem cells: Biology and therapeutic implications. Int J Biochem Cell Biol. 2019 Feb;107:38-52. doi: 10.1016/j.biocel.2018.12.001. Epub 2018 Dec 5
41. Paola Rizzo; Haixi Miao; Gwendolyn D'Souza; Clodia Osipo; Jieun Yun; Huiping Zhao; Joaquina Mascarenhas; Debra Wyatt; Giovanni Antico; Lu Hao; Katharine Yao; Prabha Rajan; Chindo Hicks; Kalliopi Siziopikou; Suzanne Selvaggi; Amina Bashir; Deepali Bhandari; Adriano Marchese; Urban Lendahl; Jian-Zhong Qin; Debra A. Tonetti; Kathy Albain; Brian J. Nickoloff; Lucio Miele. Cross-talk between Notch and the Estrogen Receptor in Breast Cancer Suggests Novel Therapeutic Approaches. Cancer Res (2008) 68 (13): 5226–5235.
42. Antonio Pannuti; Kimberly Foreman; Paola Rizzo; Clodia Osipo; Todd Golde; Barbara Osborne; Lucio Miele. Targeting Notch to Target Cancer Stem Cells. Clin Cancer Res (2010) 16 (12): 3141–3152.

43. James Briscoe, Pascal P Thérond. The mechanisms of Hedgehog signalling and its roles in development and disease.Nat Rev Mol Cell Biol 2013 Jul;14(7):416-29.doi: 10.1038/nrm3598.
44. Takebe, N., Miele, L., Harris, P.J., Jeong, W., Bando, H., Kahn, M., Yang, S.X., Ivy, S.P., 2015. Targeting Notch, Hedgehog, and Wnt pathways in cancer stem cells: clinical update. Nat. Rev. Clini. Oncol. 8, 445-464
45. Yamanaka S. Induction of pluripotent stem cells from mouse fibroblasts by four transcription factors. Cell Prolif 2008;41:51-6.
46. Chang CC, Shieh GS, Wu P, Lin CC, Shiau AL, Wu CL. Oct-3/4 expression reflects tumor progression and regulates motility of bladder cancer cells. *Cancer Res.* 2008;68(15):6281–6291.
47. Hu T, Liu S, Breiter DR, Wang F, Tang Y, Sun S. Octamer 4 small interfering RNA results in cancer stem cell-like cell apoptosis. Cancer Res 2008; 68(16):6533-6540
48. Gwak JM, Kim M, Kim HJ, Jang MH, Park SY. Expression of embryonal stem cell transcription factors in breast cancer: Oct4 as an indicator for poor clinical outcome and tamoxifen resistance. Oncotarget. 2017; 8(22):36305–36318
49. Reynolds BA, Weiss S. Clonal and population analyses demonstrate that an EGFresponsive mammalian embryonic CNS precursor is a stem cell. Developmental biology. 1996;175(1):1–13.
50. Gabriela Dontu, Wissam M Abdallah, Jessica M Foley, Kyle W Jackson, Michael F Clarke, Mari J Kawamura, Max S Wicha. In Vitro Propagation and Transcriptional Profiling of Human Mammary (Stem/Progenitor Cells. Genes Dev, 17 (10) 1253-70
51. Suruchi Mittal , Nicola J Brown , Ingunn Holen . The breast tumor microenvironment: role in cancer development, progression and response to therapy. Expert Rev Mol Diagn. 2018 Mar;18(3):227-243. doi: 10.1080/14737159.2018.1439382.
52. Wolfe JN. Breast patterns as an index of risk for developing breast cancer. AJR Am. J. Roentgenol. Jun 1976, 126(6): 1130-1137.
53. Hanahan D, Coussens LM. Accessories to the crime: functions of cells recruited to the tumor microenvironment. Cancer Cell. March 2012, 20;21(3): 309-22. Comprehensive overview of the contribution of the different stromal components to tumour development.
54. Frühbeck G. Overview of adipose tissue and its role in obesity and metabolic disorders. *Methods Mol Biol.* (2008) 456:1–22. 10.1007/978-1-59745-245-8_1
55. Vittoria D'Esposito, Maria Rosaria Ambrosio, Mario Giuliano, Serena Cabaro, Claudia Miele, Francesco Beguinot, and Pietro Formisano. Mammary Adipose Tissue Control of Breast Cancer Progression: Impact of Obesity and Diabetes. Front Oncol. 2020; 10: 1554. doi: 10.3389/fonc.2020.01554
56. Nieman KM, Romero IL, Van Houten B, Lengyel E. Adipose tissue and adipocytes support tumorigenesis and metastasis. Biochim Biophys Acta 2013;1831(10):1533-41.

57. D'Esposito V, Passaretti F, Hammarstedt A, Liguoro D, Terracciano D, Molea G, Canta L, Miele C, Smith U, Beguinot F, Formisano P. Adipocyte-released insulinlike growth factor-1 is regulated by glucose and fatty acids and controls breast cancer cell growth in vitro. Diabetologia. 2012 Oct;55(10):2811-22.
58. D'Esposito V, Liguoro D, Ambrosio MR, Collina F, Cantile M, Spinelli R, Raciti GA, Miele C, Valentino R, Campiglia P, De Laurentiis M, Di Bonito M, Botti G, Franco R, Beguinot F, Formisano P. Adipose microenvironment promotes triple negative breast cancer cell invasiveness and dissemination by producing CCL5. Oncotarget. 2016 Apr 26;7(17):24495-509
59. Ambrosio MR, D'Esposito V, Costa V, Liguoro D, Collina F, Cantile M, Prevete N, Passaro C, Mosca G, De Laurentiis M, Di Bonito M, Botti G, Franco R, Beguinot F, Ciccodicola A, Formisano P. Glucose impairs tamoxifen responsiveness modulating connective tissue growth factor in breast cancer cells. Oncotarget. 2017 Nov 20;8(65):109000-109017.
60. Friedenstein, A., Gorskaja, J., & Kulagina, N. (1976). Fibroblast precursor in normal and irradiated mouse hematopoietic organs. Exp Hematol., 4: 267-74.
61. Lazennec G, Jorgensen C. Concise review: adult multipotent stromal cells and cancer: risk or benefit? Stem Cells. 2008; 26(6):1387–94. DOI: 10.1634/stemcells.2007-1006
62. Minguell, J.J, Erices, A., & Conget, P. (2001). Mesenchymal stem cells. Exp Biol Med (Maywood), 226: 507-20.
63. Spees, JL., Olson, SD., Ylostalo, J., Lynch, P., Smith, J., Perry, A.,Prockop, D. (2003). Differentation, cell fusion, and nuclear fusion during ex vivo repair of ephitelium by human adult stem cells from bone marrow stroma. *Proc Natl Acad Sci USA*, 100: 2397-402.
64. Le Blanc K, Ringden O. Immunobiology of human mesenchymal stem cells and future use in hematopoietic stem cell transplantation. Biol Blood Marrow Transplant. 2005; 11(5):321–34. DOI: 10.1016/j.bbmt.2005.01.005
65. Pittenger MF, Martin BJ. Mesenchymal stem cells and their potential as cardiac therapeutics. Circ Res. 2004; 95(1):9–20. DOI: 10.1161/01.RES.0000135902.99383.6
66. Ridge SM, Sullivan FJ, Glynn SA. Mesenchymal stem cells: key players in cancer progression. Mol Cancer. 2017; 16(1):31.doi: 10.1186/s12943-017-0597-8
67. Lazennec G, Lam PY. Recent discoveries concerning the tumor - mesenchymal stem cell interactions. Biochim Biophys Acta. 2016; 1866(2):290–299. DOI: 10.1016/j.bbcan.2016.10.004
68. Walter M, Liang S, Ghosh S, Hornsby PJ, Li R. Interleukin 6 secreted from adipose stromal cells promotes migration and invasion of breast cancer cells. Oncogene. 2009;28:2745–2755.
69. Martin TA, Parr C, Davies G, Watkins G, Lane J, Matsumoto K, Nakamura T, Mansel RE, Jiang WG. Growth and angiogenesis of human breast cancer

in a nude mouse tumour model is reduced by NK4, a HGF/SF antagonist. Carcinogenesis. 2003;24:1317–1323.
70. Beckermann BM, Kallifatidis G, Groth A, Frommhold D, Apel A, Mattern J, Salnikov AV, Moldenhauer G, Wagner W, Diehlmann A, Saffrich R, Schubert M, Ho AD, Giese N, Buchler MW, Friess H, Buchler P, Herr I. VEGF expression by mesenchymal stem cells contributes to angiogenesis in pancreatic carcinoma. Br J Cancer. 2008;99:622–631.
71. Hung SP, Yang MH, Tseng KF, Lee OK. Hypoxia-induced Secretion of TGF-beta 1 in Mesenchymal Stem Cell Promotes Breast Cancer Cell Progression. Cell Transplant. 2012
72. Ye H, Cheng J, Tang Y, Liu Z, Xu C, Liu Y, Sun Y. Human bone marrow-derived mesenchymal stem cells produced TGFbeta contributes to progression and metastasis of prostate cancer. Cancer Invest. 2012;30:513–518.
73. Xu J, Lamouille S, Derynck R. TGF-beta-induced epithelial to mesenchymal transition. Cell Res. 2009;19:156–172.
74. Zhang Y, Yao F, Yao X, Yi C, Tan C, Wei L, Sun S. Role of CCL5 in invasion, proliferation and proportion of CD44+/CD24− phenotype of MCF-7 cells and correlation of CCL5 and CCR5 expression with breast cancer progression. Oncol Rep. 2009;21:1113–1121.
75. Tomasek, J. J., Gabbiani, G., Hinz, B., Chaponnier, C. & Brown, R. A. Myofibroblasts and mechano-regulation of connective tissue remodelling. Nature Rev. Mol. Cell Biol. 3, 349–363 (2002).
76. Chang, H. Y. et al. Diversity, topographic differentiation, and positional memory in human fibroblasts. Proc. Natl Acad. Sci. USA 99, 12877–12882 (2002).
77. Sappino, A. P., Skalli, O., Jackson, B., Schurch, W. & Gabbiani, G. Smooth-muscle differentiation in stromal cells of malignant and non-malignant breast tissues. Int. J. Cancer 41, 707–712 (1988)
78. Dimanche-Boitrel, M. T. et al. In vivo and in vitro invasiveness of a rat colon-cancer cell line maintaining E-cadherin expression: an enhancing role of tumor-associated myofibroblasts. Int. J. Cancer 56, 512–521 (1994).
79. Orimo A., Gupta P.B., Sgroi D.C., Arenzana-Seisdedos F., Delaunay T., Naeem R., Carey V.J., Richardson A.L., and Weinberg R.A. (2005). Stromal fibroblasts present in invasive human breast carcinomas promote tumor growth and angiogenesis through elevated SDF-1/CXCL12 secretion. Cell 121: 335-348.
80. Huang M., Li Y., Zhang H., and Nan F. (2010). Breast cancer stromal fibroblasts promote the generation of CD44+CD24- cells through SDF-1/CXCR4 interaction. J. Exp. Clin. Cancer Res. 29: 80.
81. Paulsson J, Micke P. Prognostic relevance of cancer-associated fibroblasts in human cancer. Semin Cancer Biol 2014;25:61–8.
82. Erez, N., Truitt, M., Olson, P., Arron, S., & Hanahan, D. (2010). Cancer-Associated Fibroblasts Are Activated in Incipient Neoplasia to Orchesterate Tumor-Promoting Inflammation in an NF-KB-Dependent Manner. *Cancer Cell*, 17: 135-47.

83. Condeelis, J., & Pollard, J. (2006). Macrophages: obligate partners for tumor cell migration, invasion and metastasis. C*ell*, 124: 263-6.

84. Tsujino T, Seshimo I, Yamamoto H, et al. Stromal Myofibroblasts predict disease recurrence for colorectal cancer. Clin Cancer Res 2007;13:2082–90

85. Yamashita M., Ogawa T., Zhang X., Hanamura N., Kashikura Y., Takamura M., Yoneda M., and Shiraishi T. (2010). Role of stromal myofibroblasts in invasive breast cancer: stromal expression of alpha-smooth muscle actin correlates with worse clinical outcome. Breast Cancer 2010: 27.

86. Tuveson D, Elyada E, Öhlund D. Fibroblast heterogeneity in the cancer wound. J Cell Biol 2014;206:1503–23.

87. Berdiel-Acer M, Sanz-Pamplona R, Calon A, et al. Differences between CAFs and their paired NCF from adjacent colonic mucosa reveal functional heterogeneity of CAFs, providing prognostic information. Mol Oncol 2014;8:1290–305.

88. Huber M, Schubert R, Peter R, et al. Fibroblast activation protein: differential expression and serine protease activity in reactive stromal fibroblasts of melanocytic skin tumors. J Investig Dermatol 2003;120:182–8.

89. Zeng, S., H. Shen, W., & Liu, L. (2018). Senescence and Cancer. Cancer Transl Med, 4: 70–4.

90. Pare, R.; Yang, T.; Shin, J.-S.; Lee, C. S. (2013). The significance of the senescence pathway in breast cancer progression. Journal of Clinical Pathology, 66(6), 491–495. doi:10.1136/jclinpath-2012-201081

91. Sherr CJ, Roberts JM. CDK inhibitors: positive and negative regulators of G1-phase progression. Genes Dev. 1999; 13:1501–1512.

92. Gil J, Peters G. Regulation of the INK4b-ARF-INK4a tumour suppressor locus: all for one or one for all. Nat. Rev. Mol. Cell Biol. 2006; 7:667–677.

93. Milanovic, M.; Fan, D.N.Y.; Belenki, D.; Dabritz, J.H.M.; Zhao, Z.; Yu, Y.; Dorr, J.R.; Dimitrova, L.; Lenze, D.; Monteiro Barbosa, I.A.; et al. Senescence-associated reprogramming promotes cancer stemness. Nature 2018, 553, 96–100.

94. Coppe JP, Patil CK, Rodier F, Sun Y, Munoz DP, Goldstein J, Nelson PS, Desprez PY, Campisi J. Senescence-associated secretory phenotypes reveal cell-nonautonomous functions of oncogenic RAS and the p53 tumor suppressor. PLoS Biol. 2008 Dec 2;6(12):2853–2868.

95. Camps J., Erdos M.R., Ried T. The role of lamin B1 for the maintenance of nuclear structure and function. Nucleus. 2015;6:8–14. doi: 10.1080/19491034.2014.1003510.

96. Lamin B1 loss is a senescence-associated biomarker. Mol. Biol. Cell. 2012;23:2066–2075. doi: 10.1091/mbc.e11-10-0884.

97. Simos G, Segref A, Fasiolo F, Hellmuth K, Shevchenko A, Mann M, Hurt EC. The yeast protein Arc1p binds to tRNA and functions as a cofactor for the methionyl- and glutamyl-tRNA synthetases. EMBO J. 1996 Oct 1;15(19):5437–5448.

98. Korkaya H, Liu S, Wicha MS. Breast cancer stem cells, cytokine networks, and the tumor microenvironment. J Clin Invest. 2011 Oct;121(10):3804–3809.
99. Tsuyada A, Chow A, Wu J, Somlo G, Chu P, Loera S, Luu T, Li AX, Wu X, Ye W, Chen S, Zhou W, Yu Y, Wang YZ, Ren X, Li H, Scherle P, Kuroki Y, Wang SE. CCL2 mediates cross-talk between cancer cells and stromal fibroblasts that regulates breast cancer stem cells. Cancer Res. 2012 Jun 1;72(11):2768–2779.
100. Ishrat Rahman, Md Tanwir Athar, and Mozaffarul Islam2. Type 2 Diabetes, Obesity, and Cancer Share Some Common and Critical Pathways. Front Oncol. 2021 Jan 20. doi: 10.3389/fonc.2020.600824
101. Liao S., Li J., Wei W., Wang L., Zhang Y., Li J., Wang C., Sun S. Association between diabetes mellitus and breast cancer risk: A meta-analysis of the literature. Asian Pac. J. Cancer Prev. 2011;12:1061–1065.
102. Jie Qiu, Qinghui Zheng , Xuli Meng. Hyperglycemia and Chemoresistance in Breast Cancer: From Cellular Mechanisms to Treatment Response. Frontiers in onoclogy. 25 February 2021 doi: 10.3389/fonc.2021.628359
103. Hou Y, Zhou M, Xie J, Chao P, Feng Q, Wu J. High glucose levels promote the proliferation of breast cancer cells through GTPases. Breast Cancer (2017) 9:429–36. doi: 10.2147/BCTT.S135665
104. Stern JH, Rutkowski JM, Scherer PE. Adiponectin, leptin, and fatty acids in the maintenance of metabolic homeostasis through adipose tissue crosstalk. Cell Metab. 2016;23:770–84.
105. Dominici M, Le Blanc K, Mueller I, Slaper-Cortenbach I, Marini F, Krause D, Deans R, Keating A, Prockop D, Horwitz E. Minimal criteria for defining multipotent mesenchymal stromal cells. The International Society for Cellular Therapy position statement. Cytotherapy. 2006; 8:315–317. [PubMed: 16923606]
106. D'Esposito V, Passaretti F, Hammarstedt A, Liguoro D, Terracciano D, Molea G, Canta L, Miele C, Smith U, Beguinot F, Formisano P. Adipocyte-released insulin- like growth factor-1 is regulated by glucose and fatty acids and controls breast cancer cell growth in vitro. Diabetologia. 2012 Oct;55(10):2811-22.
107. Xupeng Bai, Jie Ni, Julia Beretov, Peter Graham, Yong Li. Cancer stem cell in breast cancer therapeutic resistance. Cancer Treat Rev. 2018 Sep;69:152-163. doi: 10.1016/j.ctrv.2018.07.004.
108. Ping Zhang, Lei Liu, Lu Zhang, Xiaogan He, Xiaojun Xu, Yaojuan Lu, Feifei Li. Runx2 is required for activity of CD44+/CD24-/low breast cancer stem cell in breast cancer development. Am J Transl Res 2020 May 15;12(5):2305-2318.
109. Seymour, T.; Twigger, A.J.; Kakulas, F. Pluripotency Genes and Their Functions in the Normal and Aberrant Breast and Brain. Int.J. Mol. Sci. 2015, 16, 27288–27301.
110. Zhang, Q.; Han, Z.; Zhu, Y.; Chen, J.; Li, W. The Role and Specific Mechanism of OCT4 in Cancer Stem Cells: A Review. Int. J.Stem Cells 2020, 13, 312–325.

111. Paraic A Kenny, Genee Y Lee, Connie A Myers, Richard M Neve, Jeremy R Semeiks, Paul T Spellman, Katrin Lorenz, Eva H Lee, Mary Helen Barcellos-Hoff, Ole W Petersen, Joe W Gray, Mina J Bissell. The morphologies of breast cancer cell lines in three-dimensional assays correlate with their profiles of gene expression. Mol Oncol. 2007 Jun;1(1):84-96. doi: 10.1016/j.molonc.2007.02.004.
112. Gokhan Bahcecioglu 1, Gozde Basara 1, Bradley W Ellis 2, Xiang Ren 1, Pinar Zorlutuna 3. Breast cancer models: Engineering the tumor microenvironment. Acta Biomater 2020 Apr 1;106:1-21. doi: 10.1016/j.actbio.2020.02.006.
113. Seymour, T.; Twigger, A.J.; Kakulas, F. Pluripotency Genes and Their Functions in the Normal and Aberrant Breast and Brain. Int. J. Mol. Sci. 2015, 16, 27288–2730]
114. Mishra P.J., Mishra P.J., Humeniuk R., Medina D.J., Alexe G., Mesirov J.P., Ganesan S., Glod J.W., and Banerjee D. (2008). Carcinoma-associated fibroblastlike differentiation of human mesenchymal stem cells. Cancer Res 68: 4331-4339.
115. Pravin J. Mishra,1,* Prasun J. Mishra,1,2,*† Rita Humeniuk,1,2,‡ Daniel J. Medina,1 Gabriela Alexe,3 Jill P. Mesirov,3 Sridhar Ganesan,1,2 John W. Glod,2,4 and Debabrata Banerjee1,2. Carcinoma Associated Fibroblast Like Differentiation of Human Mesenchymal Stem Cells. Cancer Res. 2008 Jun 1; 68(11): 4331–4339.doi: 10.1158/0008-5472.CAN-08-0943
116. Xiaoli Zhang, Kimerly Powell and Lang Li. Breast Cancer Stem Cells: Biomarkers, Identification and Isolation Methods, Regulating Mechanisms, Cellular Origin, and Beyond. Cancers. 14 December 2020
117. Byungjin Hwang, Ji Hyun Lee and Duhee Bang. Single-cell RNA sequencing technologies and bioinformatics pipelines. Exp Mol Med. 2018 Aug 7;50(8):1-14. doi: 10.1038/s12276-018-0071-8
118. Lili Ren, Junyi Li, Chuhan Wang, Zheqi Lou, Shuangshu Gao, Lingyu Zhao, Shuoshuo Wang, Anita Chaulagain, Minghui Zhang, Xiaobo Li, Jing Tang. Single-cell RNA sequencing for breast cancer: present and future. Cell Death Discov. 2021 May 14;7(1):104. doi: 10.1038/s41420-021-00485-1.
119. Shogo Kumagai, Shohei Koyama & Hiroyoshi Nishikawa. Antitumour immunity regulated by aberrant ERBB family signalling. Nature Reviews Cancer volume 21, pages181–197 2021
120. Yi-Lei Zhang, Ruo-Chen Wang, Ken Cheng, Brian Z. Ring, Li Su. Roles of Rap1 signaling in tumor cell migration and invasion. Cancer Biol Med 2017. doi: 10.20892/j.issn.2095-3941.2016.0086
121. Takebe, N., Miele, L., Harris, P.J., Jeong, W., Bando, H., Kahn, M., Yang, S.X., Ivy, S.P., 2015. Targeting Notch, Hedgehog, and Wnt pathways in cancer stem cells: clinical update. Nat. Rev. Clini. Oncol. 8, 445-464
122. Korkaya, H., Paulson, A., Iovino, F., Wicha, M.S., 2008. HER2 regulates the mammary stem/progenitor cell population driving tumorigenesis and invasion. Oncogene. 27, 6120-6130
123. Takebe, N., Harris, P.J., Warren, R.Q., Ivy, S.P., 2011. Targeting cancer stem cells by inhibiting Wnt, Notch, and Hedgehog pathways. Nat. Rev. Clin. Oncol. 8, 97-106.https://doi.org/ 10.1038/nrclinonc.2010.196.

Dottorando	**Dr.ssa Teresa Migliaccio**
Tutor	**Prof. Pietro Formisano**
Coordinatore	**Prof. Francesco Beguinot**
Corso di Dottorato	**Dottorato di Ricerca in Medicina Clinica e Sperimentale**
Ciclo	**35°**
Codice borsa	**DOT1318210 - Borsa 2**
CUP	**E65F19001220007**
Titolo Progetto	**Meccanismi molecolari alla base dell'associazione tra malattie metaboliche e carcinoma mammario ed identificazione di nuovi marcatori prognostici**

La borsa di dottorato è stata cofinanziata con risorse del
Programma Operativo Nazionale Ricerca e Innovazione 2014-2020 (CCI 2014IT16M2OP005),
Fondo Sociale Europeo, Azione I.1 "Dottorati Innovativi con caratterizzazione Industriale"